

Galactic Disc Dynamics and Structure Analysis of the Phase Spiral and Vertical Scale-heights

Alinder, Simon

2025

Document Version: Peer reviewed version (aka post-print)

Link to publication

Citation for published version (APA): Alinder, S. (2025). Galactic Disc Dynamics and Structure: Analysis of the Phase Spiral and Vertical Scale-heights. [Doctoral Thesis (compilation), Astrophysics]. Lund University.

Total number of authors:

General rights

Unless other specific re-use rights are stated the following general rights apply:

Copyright and moral rights for the publications made accessible in the public portal are retained by the authors and/or other copyright owners and it is a condition of accessing publications that users recognise and abide by the legal requirements associated with these rights.

• Users may download and print one copy of any publication from the public portal for the purpose of private study

- You may not further distribute the material or use it for any profit-making activity or commercial gain
 You may freely distribute the URL identifying the publication in the public portal

Read more about Creative commons licenses: https://creativecommons.org/licenses/

Take down policy

If you believe that this document breaches copyright please contact us providing details, and we will remove access to the work immediately and investigate your claim.

Download date: 31. Oct. 2025

Galactic Disc Dynamics and Structure

Analysis of the Phase Spiral and Vertical Scale-heights

Simon Alinder



Thesis for the degree of Doctor of Philosophy

Thesis advisors: Dr. Thomas Bensby, Dr. Paul McMillan Faculty opponent: Dr. Chervin Laporte

To be presented, with the permission of the Faculty of Science of Lund University, for public criticism in the Rydberg lecture hall at the Department of Physics on Friday, the 21st of November 2025 at 09:00.

	1				
Organization LUND UNIVERSITY	Document name DOCTORAL DISSERTA	TION			
Division of Astrophysics	Date of issue				
Department of Physics	2025-11-21				
Box 188, SE–221 00 LUND, Sweden	Sponsoring organization				
Author(s)	+				
Simon Alinder					
Title and subtitle Galactic Disc Dynamics and Structure: Analysis of t	Title and subtitle Galactic Disc Dynamics and Structure: Analysis of the Phase Spiral and Vertical Scale-heights				
Abstract					
The Milky Way provides the most detailed labor cesses of galaxy formation and evolution. Modern have revolutionised this field by revealing the exbut dynamically active and rich in non-equilibrium Understanding these structures, and how they relified of Galactic archaeology — the reconstruction in its structures and stars. This thesis investigates the structure and dynami from <i>Gaia</i> and spectroscopic data from the APOG	large-scale surveys, most tent to which the Galaxy n features that preserve tr ate to the Galaxy's broade of the Milky Way's past fro	notably the Gaia mission, is not a steady system, aces of past interactions. In this thin the evidence preserved ay using astrometric data			
phase spiral in the Galactic disc and assess how different methods of stellar classification affect our understanding of the Galaxy's large-scale structure.					
The first paper presented in this thesis analyses the Gaia phase spiral, a characteristic pattern in the vertical positions and motions of stars, and quantifies its strength and rotation across the disc using a new model. The results show that the spiral is a rotating feature whose amplitude increases with angular momentum. The second paper investigates the two-armed phase spiral observed near the Solar neighbourhood, measures its geometry and rotation and explores whether it represents a single two-armed perturbation or two overlapping ones.					
The third paper compares several methods for separating the thin and thick discs based on chemistry, kinematics, dynamics, and stellar ages. The comparison shows that the detailed properties of the components depend on the chosen method, underscoring the need for clarity in the selection of definitions.					
Key words Galactic dynamics, Galactic structure					
Classification system and/or index terms (if any)					
Supplementary bibliographical information		Language English			
ISSN and key title		978-91-8104-618-2 (print) 978-91-8104-619-9 (pdf)			
Recipient's notes	Number of pages 127	Price			
	Security classification				
I, the undersigned, being the copyright owner of the abs all reference sources the permission to publish and disse					

Date ____2025-10-8

Signature _____

Galactic Disc Dynamics and Structure

Analysis of the Phase Spiral and Vertical Scale-heights

Simon Alinder



Faculty Opponent

Dr. Chervin Laporte LIRA, Paris Observatory Meudon, France

Evaluation Committee

Prof. Daisuke Kawata Department of Space & Climate Physics, University College London London, United Kingdom

Prof. Kirsten Knudsen Department of Space, Earth and Environment, Chalmers University Göteborg, Sweden

Prof. Urban Eriksson Department of Physics and Astronomy; Physics Education Research, Uppsala University Uppsala, Sweden

Cover illustration front: An interacting pair of galaxies, showing a part of the process of galaxy formation. The effects of the interaction are visible in several ways. The disc of the larger galaxy is visibly bent and distorted, a faint stream of stars is extending from the smaller object, and a stream of matter is linking the two galaxies together. The galaxies in the image are NGC 169 and IC 1559, and the pair is called Arp 282. Credit: ESA/Hubble & NASA, J. Dalcanton, Dark Energy Survey, DOE, FNAL/DECam, CTIO/NOIRLab/NSF/AURA, SDSS Acknowledgement: J. Schmidt

Funding information: This thesis work was financially supported by the Swedish Research Council (grants 2018-04857, 2021-04153).

© Simon Alinder 2025

Faculty of Science, Division of Astrophysics Department of Physics

ISBN: 978-91-8104-618-2 (print) ISBN: 978-91-8104-619-9 (pdf)

Printed in Sweden by Media-Tryck, Lund University, Lund 2025









Contents

	List of publications
	Popular summary
	Populärvetenskaplig sammanfattning
1	Introduction
	1 The structure of the Milky Way
	2 Formation history
	3 Aim of this thesis
2	Galactic Archaeology 1
	1 Measuring the heavens
	2 Chemical composition
	3 Ages of stars
3	The phase spiral
	1 Measuring the phase spiral
	2 Quantifying the phase spiral
	The two-armed phase spiral
4	Scale-heights of the Milky Way discs
	1 Disc model
	2 Selection methods
	3 Scale parameters
5	Discussion and Outlook 45
	1 Paper I
	2 Paper II
	3 Paper III
	4 Outlook
Sc	ientific publications 59
	Author contributions
	Paper 1: Investigating the amplitude and rotation of the phase spiral in the Milky
	Way outer disc

Paper 11: Limitations and rotation of the two-armed phase spiral in the Milky	
Way stellar disc	81
Paper III: Vertical scale heights of the Milky Way thick and thin discs using	
different selection methods	95

List of publications

This thesis is based on the following publications, referred to by their Roman numerals:

Investigating the amplitude and rotation of the phase spiral in the Milky Way outer disc

```
S. Alinder, P. J. McMillan, T. Bensby
Astronomy & Astrophysics, Volume 678, id.A46, 17 pp. (2023)
```

II Limitations and rotation of the two-armed phase spiral in the Milky Way stellar disc

```
S. Alinder, P. J. McMillan, T. Bensby
Astronomy & Astrophysics, Volume 690, id.A15, 11 pp. (2024)
```

Vertical scale heights of the Milky Way thick and thin discs using different selection methods

S. Alinder, T. Bensby, P. J. McMillan Astronomy & Astrophysics, to be submitted

Papers I and II have been published under a CC-BY 4.0 license.

Popular summary

Imagine a calm pond with a flat surface. If you drop a stone into this pond, the surface will be set in motion by waves that move out from the point where the stone hit. The field I have done this thesis in, Galactic Archaeology, is like looking at a still image of a pond with a rippled surface after many impacts, both large and small, and trying to figure out which stones caused which waves, how big they were, when they hit the surface, and ideally being able to determine which of the stones that you can (maybe) see on the bottom corresponds to which hits. And the pond is also a whirlpool. And the image you are looking at is quite low resolution. It may sound hopeless, and it is definitely a large and complex task, but remarkably good results have been achieved nonetheless. Such a task is best solved by attacking it from two sides. You need to take a careful accounting of all the disturbances, patterns, and structures you can identify, while also working on creating models, simulations of the system you are trying to describe. When the results from a simulation agree with your description of the system, you can believe that you have found an explanation for your observations.

In my research, I have not worked with puddles of water but with our Galaxy, the Milky Way. I have taken on the role of a cartographer who examines different structures in our Galaxy. My first two papers were about a spiral pattern in the stars of our Galaxy, not a physical pattern in their location, but a pattern in their movements upwards and downwards. Some of the stars in the Milky Way's disc move as if in a wave pattern, although we cannot see it because the movement occurs on time scales of tens to hundreds of millions of years. This pattern is called a phase spiral and has only been known about since 2018, so there is still much to discover and understand about it. In my first paper, I showed how the spiral pattern seems to rotate along the Milky Way's disc and that the pattern becomes stronger further out in the disc, and I developed a way to measure the properties of the spiral pattern. In my second paper, I focused on stars that are currently at the farthest point in their orbits around the Galaxy and near the Sun, meaning they spend most of their time closer to the Galaxy's core. When you do the same studies among these stars, to see the phase spiral, you see a spiral pattern with two arms. I investigated whether this is a phenomenon among these slow stars in general or whether it only affects stars in a certain range of velocities. To my surprise, I found that no two-armed spiral pattern could be seen in stars with lower velocities than those already known. No one knows yet why this is the case. In the same paper, I was also able to demonstrate that the two-armed spiral also appears to rotate along the disc of the Galaxy.

When measuring stellar densities in the Milky Way's disc, the way the density of the stars decreases with height does not match any simple function, but it does match the sum of two exponential functions. Therefore, it seems natural to divide it into two components, a thick disc and a thin disc. There are several different proposed formation scenarios for the

thick disc, and it is unclear which is the correct one. One of the most popular theories is that the thick disc formed first and experienced some kind of major disruption early in the Milky Way's history, where it was dispersed into a more diffuse shape, and that the thin disc formed afterwards, during a calmer period. The discs overlap to a large extent, but because of their different origins, there are ways to determine whether a given star belongs to one or the other. We tried categorising stars by their chemical composition, motion, orbit, and age. These different methods give similar but not identical selections, and which method you choose will affect which version of the thin or thick disc you will see. For example, the thick disc is more extended if you define it according to the positions of the stars than if you define it according to the chemical composition of the stars. Therefore, it is important to have this kind of comparative study, to point out and show differences that a research study can assume before even getting results, just from how you choose to define your question.

Populärvetenskaplig sammanfattning

Föreställ er en lugn damm med en blank yta. Om man släpper en sten i denna damm kommer ytan sättas i svängning av vågor som rör sig ut från punkten där stenen träffade. Fältet jag har gjort denna avhandling inom, Galaktisk arkeologi, är som att titta på en stillbild av en damm med krusig yta efter många nerslag, både stora och små, och försöka räkna ut vilka stenar som orsakat vilka vågor, hur stora dom var, när dom träffade ytan, och helst kunna avgöra vilken av stenarna som man (kanske) ser på bottnen som motsvarar vilken träff. Och dammen är också en strömvirvel. Och bilden du tittar på är ganska lågupplöst. Det låter kanske hopplöst, och det är definitivt en stor och komplex uppgift, men anmärkningsvärt goda resultat har ändå nåtts. En sådan uppgift löses bäst genom angrepp från två håll, man behöver både göra en noggrann kartläggning av alla störningar, mönster och strukturer man kan identifiera, samtidigt som man också jobbar på att skapa modeller, simuleringar, av det system man försöker beskriva. När resultaten från en simulering stämmer överens med ens beskrivning av systemet kan man tro att man har hittat en förklaring till sina observationer.

I min forskning har jag inte jobbat med vattenpölar utan med vår galax Vintergatan. Jag har tagit på mig rollen som kartläggare som undersöker olika strukturer i vår galax. Mina första två artiklar handlade om ett spiralmönster i galaxens stjärnor, inte ett fysiskt mönster i deras plats utan ett mönster i deras rörelser i höjdled. En del av stjärnorna i Vintergatans skiva rör sig som i ett vågmönster, fast vi kan inte se rörelsen på grund av att den sker under tiotals till hundratals millioner år. Detta mönster kallas för en fas-spiral och har bara varit känt sedan 2018 så det finns ännu mycket att upptäcka och förstå om det. I min första artikel visade jag hur spiralmönstret har olika rotation på olika platser längs Vintergatans skiva och att mönstret blir starkare längre ut i skivan samt att jag utvecklade en metod för att mäta spiralmönstrets egenskaper. I min andra artikel fokuserade jag på stjärnor som i solens närhet är längst ut i sin bana runt galaxen, de spenderar alltså resten av sin tid närmare galaxens kärna. När man gör samma undersökningar bland dessa stjärnor, för att se fas-spiralen, så ser man ett spiralmönster med två armar. Jag undersökte huruvida detta är ett fenomen bland långsamma stjärnor i allmänhet, eller om det bara rör sig om stjärnor i ett visst spann av hastigheter. Till min förvåning fann jag att det inte gick att se något tvåarmat spiralmönster i stjärnor med lägre hastigheter än de som redan var kända. Ingen vet ännu varför så är fallet. I samma artikel kunde jag också påvisa att även den tvåarmade spiralen verkar rotera längs galaxens skiva.

När man mäter stjärntätheter i Vintergatans skiva kommer man se att stjärntätheterna i höjdled mest naturligt passar med två överlappande grupper. Därför är det vanligt att dela in skivan i två beståndsdelar, en tjock skiva och en tunn skiva. Det finns flera olika teorier för hur den tjocka skivan bildades och det är ännu oklart vilken som är sann. En av de mest populära scenariorna är att den tjocka skivan bildades först och genomgick någon form av kraftig störning tidigt i galaxens historia där den blev skingrad till en mer utspridd form,

och att den tunna skivan bildades senare, under en lungnare period. Skivorna överlappar varandra till stor del, men på grund av deras olika ursprung finns det sätt att avgöra om en given stjärna tillhör den ena eller andra. Vi testade att kategorisera stjärnor efter kemisk sammansättning, rörelser, omloppsbanor, och ålder. Dessa olika metoder ger liknande men inte identiska indelningar, och vilken metod man väljer kommer påverka vilken version av den tunna eller tjocka skivan man ser. Till exempel så är den tjocka skivan längre om man definierar den enligt stjärnornas position än om man definierar den enligt stjärnornas kemiska sammansättning. Det här gör att en forskningsstudie kan nå olika resultat utifrån hur man ställer sin fråga, och därför är det viktigt att veta hur uppdelningen kommer påverka ens svar.

Acknowledgements

Firstly, I want to thank my supervisors, Thomas Bensby and Paul McMillan, for the opportunity of this education and your support throughout, with a special thanks to Paul for continuing his help and support even after moving abroad.

Next, I want to thank my friends at Astrophysics. I especially want to extend my gratitude to the following people. Ross, for your for the social get-togethers, and for your friendliness and trust. Camilla and Isabella, for the Scandinavian language chats. Bibi, for fostering solidarity among the PhD students. Eero, for many stimulating discussions about the finer points of computers and operating systems.

I want to express my deepest gratitude to my wife Gertrud, for your enormous support in matters big and small, through good times and bad. Thank you also for proofreading all my publications, despite the subject matter lying outside your area of expertise.

Finally, I thank my family for their support, belief, and enthusiasm over the years.

Chapter 1

Introduction

1 The structure of the Milky Way

If you find yourself outside on a clear, dark night, far from city lights, and look up, you will see a band of stars so dense that they blend together into a fuzzy streak. This is the disc of the Milky Way Galaxy that you are seeing from the inside. From Sweden, we can only see the outer disc, the part that is away from the centre, and it looks like Fig. 1.1, if you are lucky. From further south, you can sometimes see the central region of the Milky Way.

The Milky Way is a barred spiral galaxy that can conceptually be divided into several different components. The major ones are the disc, which we are inside, the bulge in the central region, and the halo surrounding everything. Each of these components can be further divided. The disc is composed of a thin and a thick component (Gilmore & Reid 1983), the halo has an inner part that is made from material scattered from ancient massive mergers (Helmi et al. 2018) and an outer part made from remnants of other dwarf galaxies that have fallen into the gravitational potential of the Milky Way and been ripped apart (Helmi 2008; Chung et al. 2016). In the centre, there is not just a bulge but also a bar (Dwek et al. 1995), a not-yet-fully-understood elongated structure of stars that seems to anchor the spiral arms in the disc. These components are seen in other galaxies as well, but are harder to investigate in detail because of the great distances.

We study these components and the details of the structure of the Milky Way to gain insight into the history of our Galaxy. This discipline is called Galactic archaeology, and it seeks to piece together the history of formation and evolution of the Milky Way and other galaxies from the stars, gas, and dynamical and chemical structures we observe today. The mechanisms and processes that led to the formation of large spiral galaxies are not fully understood, and the Milky Way is the most detailed laboratory for studying how galaxies



Figure 1.1: The Milky Way disc in the night sky from the northern hemisphere.

© Giles Laurent, gileslaurent.com, License CC BY-SA 4.0 https://creativecommons.org/licenses/by-sa/4.0, via Wikimedia Commons.

form, evolve, and respond to both internal processes and external perturbers. Reconstructing the history of the Milky Way can help us answer some big questions: When did the different parts of the Galaxy, such as the thin disc, the thick disc, and the stellar halo, form? How significant were accretion events compared to internal star formation? What physical processes drove the distribution of stars and gas across the Galaxy? These are not only questions about the Milky Way, but also about galaxies in general, since many of the processes that shaped our Galaxy can be assumed to be common across the universe. Furthermore, the study of Galactic archaeology connects to other areas of astrophysics in a fundamental way. Stellar populations provide information about nucleosynthesis and the

chemical evolution of the universe. The elements present in a star's atmosphere preserve a record of the chemical composition of the gas cloud from which it formed, so by measuring the relative abundances of different elements in many stars of different ages and locations, we can reconstruct how successive generations of stars enriched the Galaxy with heavier elements. When studied together with the motions and compositions of stars, this allows us to trace ancient mergers and perturbations, which in turn help to test cosmological models of structure formation. In this way, Galactic archaeology is not a stand-alone subject, but connects to the small-scale stellar physics and the large-scale physics of the structure of the cosmos.

1.1 The thin and thick discs

The disc of the Galaxy is frequently divided into two components, the thick and the thin disc. The first time this division was made was by Gilmore & Reid (1983), who were observing stars in the direction of the Galactic south pole (down through the plane). They found they required two exponential functions to fit the observed density of stars, one decaying more slowly than the other. They called these the thick and thin discs, respectively. Since then, a lot of work has gone into further characterising these populations or trying to disprove them as real, distinct populations. The two discs each have distinct structural, kinematic, and chemical characteristics. The thick disc reaches higher above the Galactic plane with a scale height of approximately 1.0 to 1.5 kpc. The scale height is the distance after which the stellar density is reduced by a factor e. It is also less extended radially (Bensby et al. 2011; Bovy et al. 2012), its stars are older and have lower metallicities (Fuhrmann 1998; Bensby et al. 2003; Reddy et al. 2003; Katz et al. 2021). Kinematically, thick-disc stars exhibit higher velocity dispersion and slower rotation in the solar neighbourhood, called asymmetric drift, compared to the thin disc (Hayden et al. 2017). In contrast, the thin disc has a scale height of 300 to 350 pc, is more extended, younger, and more metal-rich (e.g. Bensby et al. 2005). It is kinematically colder with a lower velocity dispersion, and its rotational velocity is close to that of the Milky Way's circular speed (Casetti-Dinescu et al. 2011).

The thin disc extends further out than the thick disc and increases in thickness with distance, called the flare (Bovy et al. 2016; Mackereth et al. 2017). The disc has no distinct endpoint, it gets more and more diffuse until we can't detect it any more, and disc stars have been detected at distances of over 30 kpc (López-Corredoira et al. 2018). The thin disc is possibly the most well-studied of the Galactic components because the Sun is a part of it, orbiting at about 8 kpc from the Galactic centre. Stars in the thin disc are relatively young, and star formation is still ongoing here. There is an observable gradient in metallicity in the thin disc, with the most metal-rich stars closer to the centre and more metal-poor ones towards the outer edge (e.g., Katz et al. 2021). This is explained by the thin disc forming

inside-out, which means there was early, rapid star formation in the centre of the Galaxy, which enriched the interstellar medium, and the stars that formed from it, with heavier elements. When combined with the fact that most stars in the thin disc have formed at a different distance to the centre of the Galaxy than they exist at today, they have migrated over their lifetimes (Sellwood & Binney 2002), we can explain the change in average metallicity across the disc.

1.2 The bulge and bar

The centre of the Galaxy is thicker and contains a roughly spheroidal structure of stars called the bulge (Dwek et al. 1995). This feature can be seen from Earth in the southern hemisphere. It consists of both young and old stars (Nepal et al. 2025) and is a few kpc in radius. The bar is a large, elongated stellar structure in the centre of the Galaxy that extends past the bulge. The shape, size, and rotation of the bar have been debated for a long time, as the bar is hard to study because it is inside a region of dense dust. The properties of the bar also affect the rest of the Galaxy, particularly some of the structures in the disc that we will be interested in later.

The origin of the bulge in the Milky Way, and bulges in general, is a much-discussed topic in the scientific literature. There are three different kinds of bulges that are usually discussed (Athanassoula 2005). One is called a classical bulge (for historic reasons), and it is a spherical system similar to an elliptical galaxy in many ways, except it is surrounded by a disc. The main characteristic of this kind of bulge is that the stars in it are on orbits that are oriented randomly, leading to a theory that these systems are formed through mergers early in the history of galaxy formation, like elliptical galaxies, and their outer regions then settled into a disc (Immeli et al. 2004). The spiral arms in these discs end at the edge of the bulge. Another kind is called a pseudobulge, or sometimes a disc-like bulge. The stars in this kind of bulge are on orbits that are ordered and look more like those of stars in a disc. How this kind of bulge is formed is not completely clear, but it is thought that these bulges are formed by the disc itself as it changes over time (Kormendy & Kennicutt 2004). Finally, there are the boxy/peanut bulges. These are sometimes seen in galaxies viewed edge-on as an X- or square shape. These bulges are formed by the bar as some stars in it are moved vertically, creating the X-shape. The Milky Way has been found to contain this kind of structure (Ness & Lang 2016).

1.3 The halo

The Milky Way is, like other spiral galaxies, surrounded by a halo. This halo is roughly spherical and contains some stars as well as numerous globular clusters, stellar streams, and old low-metallicity stars. The halo is denser, and its stars move faster, closer to the centre.

The halo does not have an inner edge, and halo stars can be found in the disc as they pass through, which is relevant to consider when we want to study disc stars.

Most of the mass of the halo, and indeed the entire Galaxy, is gas and dark matter (Lundmark 1930; Rubin & Ford 1970; Bosma 1978), which is the name given to the cause of the high rotational velocities of stars in the disc. Based on only the matter that we can observe (stars, gas, dust, etc.), the stars in the disc should be orbiting more slowly than they are. Assuming this additional speed is due to there being more mass in the Galaxy than we can see, we call this hypothetical mass dark matter. There are numerous other lines of evidence for dark matter, so even though we do not know what it is, we still have reasons to believe it exists.

1.4 Other structures

The Galaxy contains a huge number of other structures, many of them known for several decades. Much progress has been made recently thanks to the space observatory *Gaia*, which has been charting the position and motion of more than two billion stars, showing us how our Galaxy is changing and evolving to this day (Gaia Collaboration et al. 2016a). While this has been known for a long time, the extent of the disequilibrium was one of the biggest realisations for the astronomical community upon receiving the first data from *Gaia*. It shows that, even though the Galaxy has evolved mostly in isolation for many billion years, the disc is still ringing, pulsing, and shaking from past interactions, large and small (Hunt & Vasiliev 2025), and the signs of this ongoing process are visible in the many smaller structures in the Galaxy.

Arguably the largest disequilibrium feature in the Galaxy is the warp. This is the bending of the disc of the Galaxy where one edge curves upwards and the other downwards, as illustrated in Fig. 1.2. This phenomenon has been known for a long time, being first discovered in the 1950s in observations of the distribution of hydrogen gas (Kerr et al. 1957; Burke 1957; Westerhout 1957). The bending of the disc starts at about 10 kpc from the Galactic centre, 2 kpc further out than the Sun, and at the edge of the Galaxy, the disc reaches over 1 kpc up or down from the mid-plane of the inner Galaxy (Cheng et al. 2020). The ultimate cause of the warp is unknown, but *Gaia* has let us study the phenomena in greater detail. *Gaia* lets us see the motions of the stars in the warp, which allows us to measure its speed of precession. The stars in the warp orbit the Galaxy faster than the warp precesses, but the warp does precess, travelling like a wave along the disc (Jónsson & McMillan 2024).

Outside of the disc, in the halo, we find stellar streams and satellite dwarf galaxies. Streams are elongated, dynamically cold filaments of stars that orbit the Milky Way, typically formed when a globular cluster or dwarf galaxy falls into the Milky Way and is disrupted by tidal

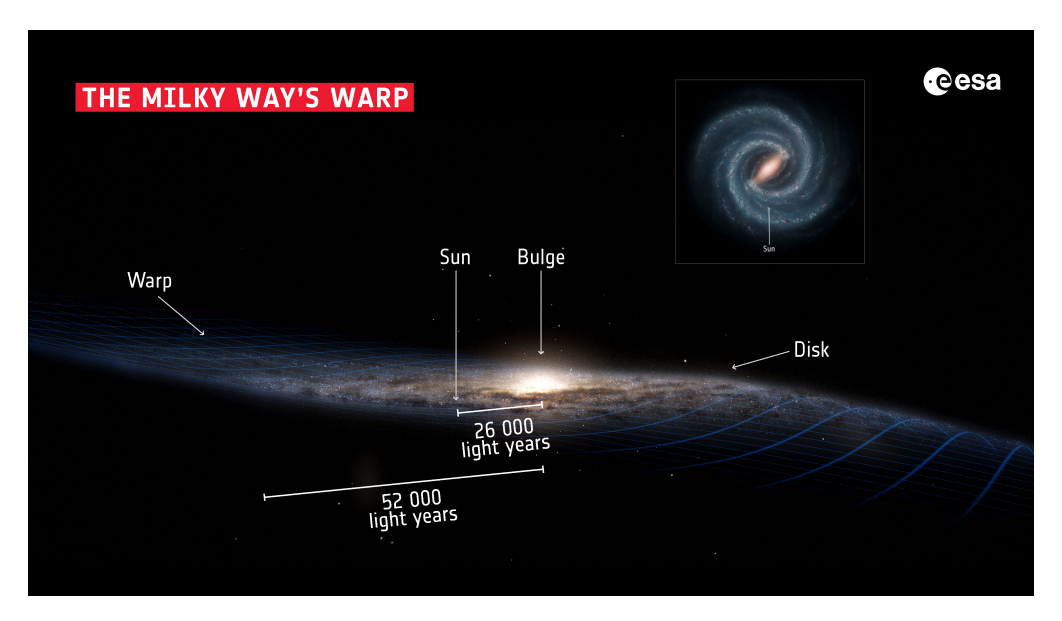


Figure 1.2: Artist impression of the Milky Way with the warped disc. Image credit: ESA/NASA

forces to have its stars drawn out along its orbit. These structures can stretch tens to hundreds of parsecs or even span great arcs across the whole Galaxy. They can serve as sensitive gravitational probes, mapping the Galactic potential and offering insights into the distribution of dark matter on small scales (Belokurov et al. 2006). The first and most well-studied example of a stream is the Sagittarius Stream, which originates from the Sagittarius dwarf galaxy (Ibata et al. 1994, 1995; Lynden-Bell & Lynden-Bell 1995). The Gaia mission has been revolutionary for the study of stellar streams by enabling the discovery and characterisation of more than one hundred of them by identifying co-moving groups in the Galactic halo (Ibata et al. 2021, 2024; Bonaca & Price-Whelan 2025). Gaia data also revealed common density variations along and across streams, signatures expected from interactions with dark-matter subhalos or baryonic structures, and provided proper motions that guide spectroscopic follow-ups (Bonaca & Price-Whelan 2025). Further out are the dwarf galaxies, the Large Magellanic Cloud and the Small Magellanic Cloud, among many others. These nearby dwarf galaxies are visible to the unaided eye from the southern hemisphere and are sure to be affecting the Galactic disc (Laporte et al. 2018), but matching observed phenomena to each dwarf galaxy has not yet been possible because our understanding of the dwarf galaxies is still incomplete.

In 2015, Xu et al. (2015) discovered that the Milky Way's disc exhibits vertical, wave-like oscillations referred to as corrugations in the Galactic anticentre direction. They detected an asymmetric pattern in stellar density above and below the Galactic mid-plane: an excess of stars north of the plane at approximately 2 kpc from the Sun, south of the plane at

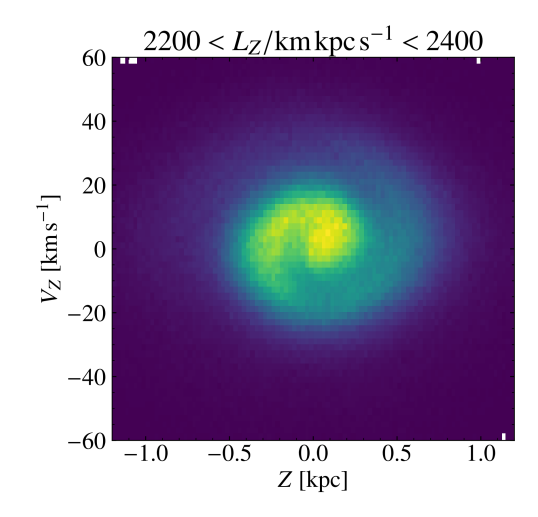


Figure 1.3: Number density of stars in the Z - V_Z phase plane, showing a spiral pattern. The stars have vertical angular momenta (L_Z) in the range 2200 - 2400 kpc km s⁻¹, placing them further out in the disc than the Sun.

4-6 kpc, and north again at 8-10 kpc, with indications of another southern excess at 12-16 kpc. These vertical displacements were modelled as concentric ripples or "rings" in the disc, offset by about 100 pc, and suggest that structures such as the Monoceros (Newberg et al. 2002; Ibata et al. 2003) and Triangulum-Andromeda (Rocha-Pinto et al. 2004) features are manifestations of these oscillations. These corrugations are large-scale, non-axisymmetric, non-equilibrium features of the Galactic disc, demonstrating that it is far from a smooth, flat structure. *Gaia*'s high-precision astrometry has since furthered this picture: it has revealed kinematic signatures of vertical and radial waves in the disc, enabled mapping of complex bending and breathing modes, and strengthened the view that the disc remains dynamically active and perturbed (Poggio et al. 2025).

One of the many discoveries to come out of the *Gaia* data is the phase spiral, often called the *Gaia* phase spiral or the phase snail. It was discovered by Antoja et al. (2018) as a spiral pattern of increased azimuthal velocity (V_{ϕ}) in the Z - V_Z phase plane, and is the subject of the first two papers in this thesis. The vertical motions of a star through the disc are captured as circular motion around the Z - V_Z phase plane, with larger vertical excursions producing wider circles. The spiral pattern means that the distribution of vertical motions in this group of stars is not uniform. It means stars are more likely to have certain vertical positions and velocities than others, as if something recently synchronised these stars. After its initial discovery, the phase spiral was detected in progressively more remote areas of the Galaxy, and we can now claim that the phase spiral is a global phenomenon in the disc. Along the way, it was found that the phase spiral depends on the dynamical properties of the stars. For example, when selecting a sample of stars to put in a Z - V_Z phase plane diagram,

the image of the phase spiral will be significantly clearer if, instead of radial distance and azimuthal angle, angular momentum and phase angle are used to define the sample. If these selection criteria are used, the spiral pattern can even show up clearly in a simple number density plot of the phase plane, such as Fig. 1.3.

There are plenty of other structures and substructures in the disc, taking the form of stars that group together in kinematic space, i.e. they have similar movements. They could be the remnants of once-coherent structures like clusters or dwarf galaxies, or they could have been excited into motion at the same time by a larger structure like the bar (Dehnen 1999; Kushniruk et al. 2017; Laporte et al. 2020b). Another example is the so-called disc streams, or "feathers", which are large and extended groups of stars that have been kicked up from the disc (Bergemann et al. 2018; Sheffield et al. 2018) by some large external force, like a passing dwarf galaxy, and studying them can lead to more insights into these events (Laporte et al. 2019a, 2020a). The feathers are associated with the Monoceros ring (Slater et al. 2014), and thus located in the outer disc. There, the gravitational potential is lower, so structures like these can persist for longer and remain for several Gyrs, giving us a window into the history of the Milky Way (Laporte et al. 2022).

2 Formation history

The purpose of studying all these structures and phenomena is to understand how the Galaxy, and galaxies in general, came to be. Galaxy formation is a major area of study in astrophysics, so here follows a brief overview of the parts of the early formation that are relevant for this thesis.

Structures like galaxies started to form in the early universe in a bottom-up manner, meaning smaller structures formed first and then came together to form larger structures (e.g., Mori & Umemura 2006). Clouds of gas came together to form stars, which then came together to form clusters, which formed galaxies. The details of this very earliest era of the formation of a disc galaxy like the Milky Way are currently unknown (Planelles et al. 2015). There is rapid progress being made with new data from, among other sources, the JWST (James Webb Space Telescope), which reveals galaxies with discs or disc-like structures earlier than was previously thought possible (e.g., Glazebrook et al. 2024; Wang et al. 2025).

An early galaxy grows through inflows of intergalactic gas and by mergers with other structures. If the incoming object is small, it will cause a minor merger which will not affect the overall structure of the galaxy, only contribute mass and add smaller structures to it. These mergers result in stellar streams, tidal tails, disturbed gas, or other phenomena that are observed in both the Milky Way and other galaxies (Martínez-Delgado et al. 2010). If

the incoming object is large enough to disrupt the existing structures of the galaxy, it will cause a major merger. These events are much rarer but can completely alter the galaxy by destroying structures and triggering the formation of new ones by disrupting the gas in the galaxy, giving more opportunities for it to collapse and cause rapid star formation (Lambas et al. 2012).

It is believed the Milky Way underwent a major merger between 8 and 10 Gyrs ago. This was probably not the first such merger, but it was the last, and it would cover the traces of any earlier ones. The primary evidence for this merger is the presence of a population of stars with different kinematic and chemical properties than the stars of the disc and halo (Belokurov et al. 2018; Helmi et al. 2018). These other stars have a slightly retrograde mean motion and significantly lower abundances of certain elements than the thick or thin disc, and more elongated orbits than the metal-poor halo. This structure, as well as the galaxy that originated it, is called Gaia-Sausage-Enceladus, often shortened to GSE. "Gaia" because this discovery was made using data from the Gaia space observatory, "Sausage" because of the characteristic shape of the population in a chart of velocity space, and "Enceladus" after the mythological giant, son of Gaia, who was buried under mount Etna and the cause of its earthquakes, shaking the world like the merger shook the Milky Way. Several other merger remnants have been discovered, though they are significantly more enigmatic since they are either smaller or older than GSE (Massari et al. 2019). The largest is called "Kraken" and is believed to have had a mass similar to GSE (Kruijssen et al. 2020) and to have merged with the young Milky Way not much earlier than GSE (Orkney et al. 2022).

The merger with GSE disrupted the disc the Milky Way had at that time. One of the leading theories for the origin of the thick disc is that the stars scattered or formed in this event eventually go on to re-form into a kinematically heated, thick disc (Helmi et al. 2018; Grand et al. 2020; Xiang & Rix 2022). After the original disc had settled down, a new disc was able to form without being disturbed, becoming the thin disc. Others argue that the thick disc formed on its own via mechanisms internal to the Galaxy without needing a major merger (Bournaud et al. 2009; Schönrich & Binney 2009; Minchev et al. 2015), though there is disagreement over the significance of processes like radial migration (Haywood et al. 2013; Khoperskov et al. 2021).

The thin and thick discs are observed to have different chemical compositions, which can be explained by them forming at different times in environments that have progressed different amounts through galactic chemical evolution. This is primarily dictated by different kinds of supernovae that happen at different stages of stellar evolution. Type II supernovae, caused by massive stars exploding at the end of their lifetimes, can happen earlier than type Ia supernovae, caused by white dwarfs accreting material until they reach a critical mass and explode (Matteucci & Greggio 1986). There is a specific class of elements that are usually given closer attention when discussing formation histories. These are called the α -elements

because they are primarily produced by the α -process. The α -elements are C, O, Ne, Mg, Si, S, Ar, and Ca, each of which has an atomic number 2 higher than the last because they are formed by the absorption of a helium nucleus, an alpha particle. Type II supernovae produce both α -elements and iron, while type Ia supernovae produce iron but essentially no α -elements (Matteucci & Greggio 1986). Because of this, we can estimate the age of the environment a star formed in by measuring its ratio of α -elements to iron.

3 Aim of this thesis

In the field of Galactic archaeology, there remain many open questions. Are we currently observing the Galaxy in a transient state, or are the perturbations we observe long-lived? What is the origin of the phase spiral? What role did radial migration play in shaping the metallicity and age distributions across the Galactic disc? How do the stars in the bulge connect chemically and dynamically to the thin and thick discs? Is the Milky Way typical compared to other disc galaxies of similar mass and morphology, or is its formation history unusual? Questions like these make this field highly receptive to further research. This thesis includes two papers on the *Gaia* phase spiral and one on the properties and shapes of the thin and thick discs. All three papers seek to chart the structures of the Galaxy and provide further information on the details of its shape, size, and behaviour.

The first part of this thesis focuses on the *Gaia* phase spiral. By determining its properties, such as its morphology, rotation, amplitude, and dependence on stellar metallicity, this research seeks to provide more data on the nature of this phenomenon to place it into a broader Galactic context. Understanding this feature not only provides constraints on the possible physical mechanisms responsible for its formation, such as satellite interactions or internal dynamical processes, but also provides information on the dynamical state of the Galactic disc as a whole, insights that are useful for reconstructing the sequence of events that shaped the present-day Milky Way. The second part of this thesis examines the large-scale structure of the Galactic disc through a comparison of different classification methods for assigning stars to the thin and thick discs. By evaluating how these methods affect the derived parameters, such as disc scale height or the proportion of thick disc stars in the mid-plane, this study aims to highlight the importance of these choices in order to ensure that the inferred properties of the disc are robust. Taken together, these studies contribute to the broader aim of charting the structure and dynamics of the Milky Way and linking them to its formation history.

Chapter 2

Galactic Archaeology

The work in this thesis can be described as Galactic archaeology, because I am looking at the current state of the Galaxy and trying to deduce what happened in the past to get us to this point. To do this work, one needs many kinds of data on the stars in our Galaxy, none of which are trivial to collect. With some modern stellar catalogues, we talk about having six-dimensional (6D) data, meaning we have complete information on the position of the star in 3D space and its 3D motion. There is a lot more information that can be learned about a star than where it is and where it is going, such as what it is made of and how old it is. One can say these would constitute additional dimensions of data, bringing us to N-dimensional data. With access to data like this, it is possible to start to piece together a history of the Galaxy. In this chapter, I will go through a very brief history of how humanity progressed to the point of gathering the wealth of data we currently have access to.

1 Measuring the heavens

1.1 Building towards 6D

The first systematic records of astronomic observations, that we know of, come from the Babylonian tablet called MUL.APIN from the 7th-century BCE, believed to be a copy of an older text from around 1000 BCE, which records a number of stars and constellations along with their times of rising and setting. The first known record of numerical positions of stars was made by Timocharis, who recorded the declination (height above or below the celestial equator) of 18 stars. Hipparchus later created a catalogue of about 850 stars for which he used instruments that were modern at the time to achieve an accuracy of about half a degree. This increase in accuracy enabled several new discoveries, such as predictions

of eclipses and, using Timocharis' data from 150 years earlier, the precession of the equinoxes. Without telescopes or other advanced instruments, it was only possible to record the coordinates of each star on the sky, a 2D measurement. Many more important catalogues were created in the following centuries (by Ulugh Beg, Chinese court astronomers, Nicolaus Copernicus, Tycho Brahe, and others), which contained improvements in the number and quality of observations. The last one of this order, Tycho Brahe's catalogue published in 1627, contained about 1000 stars with an accuracy of about 1 arc minute (Wynn-Williams 2016). The work of these early astronomers caused debates over the position of the Earth in the cosmos, with the heliocentric model laying the groundwork for the next step.

After the heliocentric model was long established, an idea for measuring the distance to another star was born. It was to measure the apparent change in position of a star against very distant background stars caused by the motion of the Earth around the Sun over the course of a year, as illustrated in Fig. 2.1. This is called parallax, and it means that, if it is possible to accurately measure this difference in position of a star, then one can compute the distance to it. Doing this adds a third component to the knowledge of the position of a star, the distance, leading to complete knowledge of the position of that star in 3D space. The parallax angle to any star in the sky is small and changes very slowly, so it is not possible to measure without appropriate equipment. Such equipment had not been invented until the 19th century, when Friedrich Bessel became the first to publish mostly accurate results of parallax measurements in 1838 (Bessel 1838), though Thomas Henderson had made successful measurements several years earlier, but his results were not published until 1839 (Henderson 1839). Both these results were of a single star, 61 Cygni for Bessel and Alpha Centauri for Henderson, and it was not until the era of photographic astronomy that results were obtained in larger numbers. The first to use such techniques was Jacobus Kapteyn, who compiled photographic observations to create a catalogue of a few hundred parallaxes in 1910 (Kapteyn & Weersma 1910).

Parallax is not the actual motion of the stars, just the apparent motion caused by the motion of the observers, us. Stars, however, do move through space and this motion across the background is called proper motion. Proper motion is continuous and linear, unlike the periodic apparent motion caused by parallax, so careful measurements of the position of a star when the Earth is in the same place on its orbit can be used to detect this motion. The first confirmed measurement of proper motion was done in 1718 by Edmond Halley when he noticed that modern, to him, recordings of the positions of stars were about half a degree different from where they had been as recorded by the ancients (Halley 1717). With photography, measurements like these became easier and by 1919, Max Wolf had a catalogue of over 1000 proper motions (Wolf 1919). Because these observations were made from the ground, through the atmosphere, they were limited to an astrometric precision of about 0.01 arcseconds. With proper motion, we add two more dimensions of knowledge to our understanding of the stars. We now know their position on the plane of the sky, which

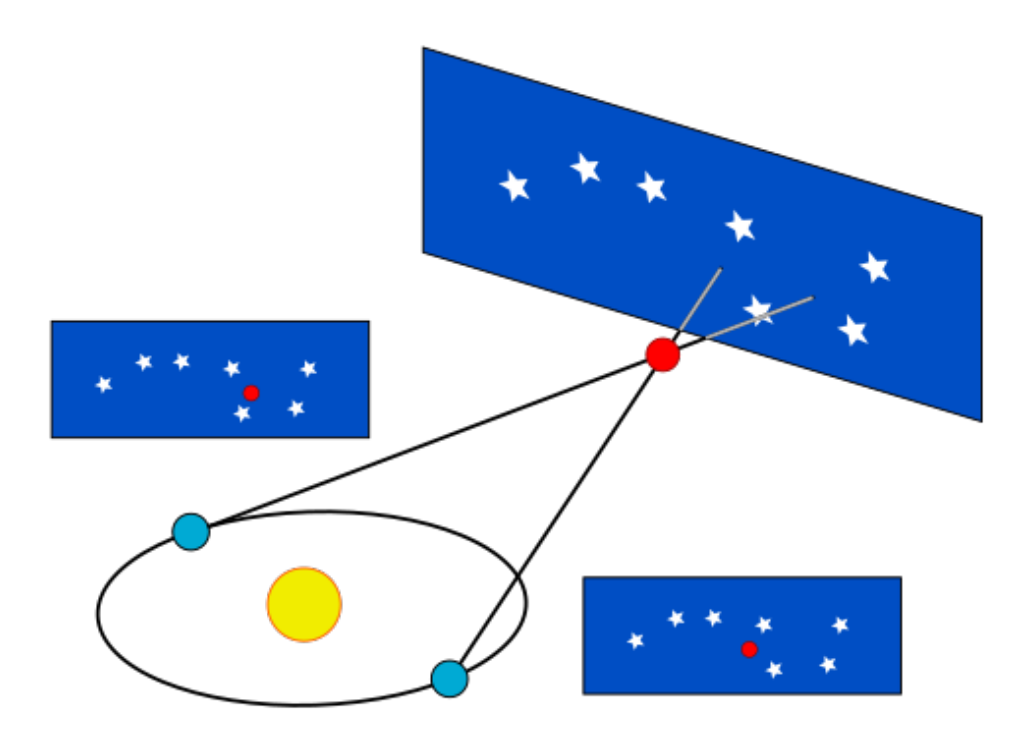


Figure 2.1: An illustration of stellar parallax. The apparent position of the red object changes with the position of the Earth in its orbit around the Sun.

KES47/Original version from German Wikipedia. By user: WikiStefan. 28 Oct 2004, CC

BY 3.0 https://creativecommons.org/licenses/by/3.0, via Wikimedia Commons.

turns into a real position in space with the distance information, and we know how they move along the plane of the sky, adding up to 5 dimensions of information. We are only lacking their motion along the line of sight to get complete knowledge of their position and motion. This presents a new kind of challenge. So far, we have been able to build up our understanding by essentially looking more closely at the stars to detect the subtleties of their positions at different times. It is not possible to detect their movement towards or away from us in this way, so a new technique is needed.

In 1868, William Huggins became the first to measure the radial velocity of a star with respect to the Sun based on the observed redshift of the star's light by measuring the Doppler shift in the sodium doublet lines at 589 nm in Sirius (Huggins 1868). His results were incorrect in both magnitude and direction, but the technique was sound and was later used to correctly measure radial velocities. Using this method, we gain the final piece of data to reach full knowledge of the 3D motion and 3D velocity of a star for a total of 6D data.

1.2 Spaceborne astrometry

Astrometry moved into space with the European Space Agency's (ESA) *Hipparcos* mission, which was operational from 1989 to 1993. It resulted in the Hipparcos catalogue of over 100 000 stars with an astrometric precision of 0.001 arcseconds (Perryman et al. 1997), and the Tycho-2 catalogue of 2.5 million stars with an astrometric precision of 0.07 arcseconds (Høg et al. 2000).

Hipparcos was a success (Perryman 2009) and led to plans for a new and better follow-up mission. This turned into the *Gaia* space observatory, which was launched by ESA in December 2013 (Gaia Collaboration et al. 2016a). It travelled to the Earth-Sun L₂ point where it conducted observations until January 2025. During this time, the spacecraft recorded the positions and brightnesses of almost 2 billion stars to great precision, representing approximately 1% of the full stellar inventory of the Milky Way.

Neither *Hipparcos* nor *Gaia* were space telescopes in the traditional sense, they did not work by taking pictures as we normally see them. They both worked by slowly spinning and using their telescopes to detect stars and measure their positions. In this way, they were able to scan the entire sky and visit each star several times, which allowed for accurate measurements of positions, proper motions and parallax (Perryman et al. 1989; Gaia Collaboration et al. 2016a).

Because the data gathered by *Gaia* is not in an immediately accessible form, it is first processed by the Data Processing and Analysis Consortium (DPAC) before being released. There have been three main data releases to date. The first one, Data Release 1 (DR1), was released in 2015 and contained data from 15 months of observations. It contained positions and magnitudes for 1.1 billion stars and positions, parallaxes and proper motions for over 2 million stars. This first data release used a combination of data from *Gaia* and the Tycho-2 catalogue from *Hipparcos* (Gaia Collaboration et al. 2016b). The second data release (DR2) was released in 2018 and used 22 months of observations. It included positions, parallaxes and proper motions (5D data) for about 1.3 billion stars and median radial velocities (6D data) for about 7.2 million stars (Gaia Collaboration et al. 2018). The third data release was split into two parts, with the first part (EDR3) being released early, in 2020, and contained data from 24 months of observations, containing 5D data for 1.4 billion stars (Gaia Collaboration et al. 2021). The full release (DR3) was released in 2022 and added 6D data for 33 million stars (Gaia Collaboration et al. 2023a).

Gaia recorded the position, brightness, and parallax of stars with precisions down to 10 microarcseconds (μ as) for positions and between 20 and 1300 μ as for parallax measurements, and achieved an uncertainty in proper motion of 20 - 1400 μ as yr⁻¹ (Gaia Collaboration et al. 2023a). Gaia also carried a high-resolution, narrow-range spectrometer for measuring radial velocities called the Radial-Velocity Spectrometer (RVS). This instrument was

designed to measure the spectral lines of calcium ions between 847 and 874 nm, which allows for the measurement of the line-of-sight velocity of stars by the Doppler shift of these lines. *Gaia* measured these radial velocities with a precision of 1.3 to 6.4 kms⁻¹ (Katz et al. 2023).

The simplest way of computing distance from parallax is by using the equation $d = \frac{1au}{b}$, where d is the distance to the star, and p is the parallax angle. If the angle is given in arcseconds, the formula can be simplified to $d=\frac{1}{p}$, and the distance will be provided in parsecs. This simple method has the weakness that it amplifies measurement errors in the parallax angle, and they act asymmetrically, with errors towards smaller angles having a larger effect than errors towards larger angles. In the ideal case of a relatively nearby bright star, this is not an issue. A star with a measured parallax of 1 mas with an error of 20 μ as will result in a distance measurement of 1 kpc (+20.4 pc, -20.6 pc), errors of +2.04% and -2.06%, respectively. For a fainter and more distant star, the situation is worse. A measured parallax of 0.1 mas (100 µas) with an error of 20 µas will result in a distance measurement of 10 kpc (+2.5 kpc, -1.66 kpc), an error of +25% or -16.7%. To get around this issue, we used distances derived using a Bayesian model that takes parallax angle, apparent magnitude, and colour into account, made by Bailer-Jones et al. (2021). Their distance estimates use the fact that the colour and absolute magnitude of a star are not independent, a given colour has a restricted range of available magnitudes, to improve their estimates.

The RVS can, despite its narrow range, be used to infer many spectral properties of a star. In our papers, we only use the estimate of the global metallicity, but the abundances of twelve different elements (N, Mg, Si, S, Ca, Ti, Cr, Fe, Ni, Zr, Ce and Nd) have been derived for 5.6 million stars from these spectra. This is possible because the spectra are high resolution and high signal-to-noise, so sufficient lines of these elements can be found and used (Recio-Blanco et al. 2023).

This wealth of data has proven to be useful for more than measuring the position and velocities of stars in the Milky Way. Massari et al. (2018) measured the motion of the nearby Sculptor dwarf galaxy, and of the stars within it. This precise accounting of the stars within the dwarf galaxy allows for more accurate models of both the visible and dark components of it, which are used to make statements on the nature of dark matter in general. The measurements of the motion of the dwarf galaxy itself allow them to determine its orbit around the Milky Way, which depends on what model for the Milky Way is used, highlighting the need for quality models. Other results range very far, from a dataset of the orbits of 157 000 asteroids in the solar system (Gaia Collaboration et al. 2023c), to a new table of quasars (Gaia Collaboration et al. 2024a), to a catalogue of the enigmatic diffuse interstellar bands (Gaia Collaboration et al. 2023b), to the discovery of three black holes found only by the peculiar motions of their companion stars and lack of a visible explanation (Tanikawa et al. 2023; El-Badry et al. 2023; Gaia Collaboration et al. 2024b).

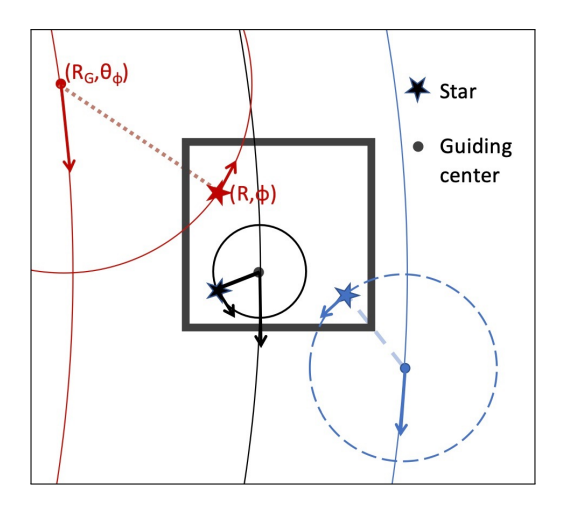


Figure 2.2: Illustration of the epicycle approximation, where the orbital motion of a star is approximated as a smaller orbit around a guiding centre that orbits the Galaxy. R_G and θ_ϕ are the coordinates of the guiding centre, and R and ϕ are the physical coordinates of the star. Stars on different orbits can be coincidentally grouped together spatially. By looking at the properties of their orbits, it is possible to make a selection based on dynamical histories instead. In order to do this, the selection can be made on the coordinates of the guiding centres instead of the coordinates of the stars.

Credit: ESCARGOT: Mapping Vertical Phase Spiral Characteristics Throughout the Real and Simulated Milky Way, Darragh-Ford et al. 2023, ApJ, 955, 74. doi.org/10.3847/1538-4357/acf1fc, licenced under CC BY 4.0.

1.3 Dynamics

All parts of this thesis use kinematics (the study of the motion of objects) to some extent. Papers II and III go deeper and use dynamics (the study of the laws governing kinematics). If we have the 6D space-velocity information about a star, we know its kinematic properties, but if we put that star into a model of the gravitational potential of the Milky Way, we can derive its dynamical properties, i.e. its orbit.

Orbits around the Milky Way are not like the nice and ordered Keplerian, closed, nearly-circular ellipses mostly in a single plane of the planets of the solar system. Even if we only consider stars in the Galactic disc, these stars are not on closed orbits so the standard Keplerian orbital elements are rarely used, because stars do not orbit around a single specific point but instead travel inside a diffuse potential made of all the other stars, gas, and dark matter of the Galaxy. To handle this complexity, a simplifying approximation is often introduced. Instead of attempting to describe the full motion directly, the motion of a star is decomposed into two parts: the circular path of an imagined point called the guiding centre around the Galaxy, and the elliptical motion of the star around this guiding centre. The distance at which the guiding centre orbits is called the guiding centre radius (R_G),

and the angular position of the guiding centre is called the phase angle (θ_{ϕ}) . This is called the epicycle approximation, illustrated in Fig. 2.2, and its usefulness lies in that, if we select stars based on location, stars that are close to each other in space at any given time may be coming from and headed in different directions, and therefore have no common history. On the other hand, if we select stars based on guiding centre radius and phase angle, we will select stars that share some history to a much larger extent. Because the epicycle approximation is only an approximation, it will break down if applied to orbits that are too far from circular (Binney & Tremaine 2008), which is why we rely on the regular action-angle coordinates for our work.

2 Chemical composition

Large amounts of information can be retrieved from stars by measuring their elemental abundances. Stellar spectroscopy is used to determine the chemical composition of a star by analysing the absorption lines in its spectrum. These lines arise when elements in the stellar atmosphere absorb specific wavelengths of light. This information can tell us about the elements that were present in the environment that the star formed in, since the composition of the visible part of the star does not change much through its lifetime, except at clear dredge-up events. By knowing the conditions a star formed in, we can group them accordingly. By tracing patterns in elemental abundances, we can even trace the history of chemical enrichment of the Galaxy. Accurately measuring the abundances of large numbers of stars is the goal of several large collaborations. Their tasks are many and difficult, usually requiring dedicated telescopes and software for consistent data processing.

We make use of spectroscopically derived chemical data for all papers in this thesis. For papers I and II, we use the global metallicity measurement derived from the Radial Velocity Spectrometer on Gaia (Recio-Blanco et al. 2023). For paper III, we use several elemental abundances from the Apache Point Observatory Galactic Evolution Experiment (APO-GEE) survey, which is a part of the larger Sloan Digital Sky Survey (SDSS) (Abdurro'uf et al. 2022). We used data from Data Release 17 (DR17), which includes data from the APOGEE-1 and APOGEE-2 component surveys. Both made spectroscopic measurements of stars in the near-infrared. APOGEE-1 used a spectrograph mounted on the Apache Point Observatory to target some 150 000 red giants in the bulge, disc, and halo during a 3-year mission (Majewski et al. 2017). APOGEE-2 added a second, almost identical, spectrograph mounted on the Irénée du Pont Telescope at Las Campanas Observatory and observed 657 000 unique targets, mostly red giants but also other types including young stars and variable stars, distributed all over the Galaxy over a 4.5-year mission (Abdurro'uf et al. 2022). The APOGEE dataset contains elemental abundances for 20 species with a precision of ~ 0.1 dex. This large number of stars with many different elemental abundances makes the APOGEE data flexible and suitable for investigating many different questions,

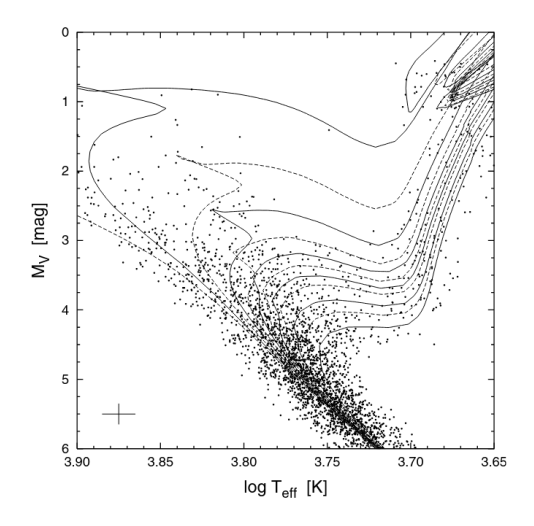


Figure 2.3: Theoretical isochrone curves computed for ages 0, 1, 2, ..., 8, 10, 12, and 15 Gyr with points representing stars.

Credit: Jørgensen & Lindegren. A&A, 436, 127, 2005, reproduced with permission © ESO.

which in turn makes it a popular source for astrophysicists to use.

3 Ages of stars

The most useful tool imaginable for Galactic archaeology would be if we could measure the ages of stars directly. Unfortunately, stars generally do not carry measurable age markers, so their ages need to be estimated from other properties. There exist several different techniques for doing so.

By placing stars in a temperature-luminosity diagram, it can be seen that most stars lie along a line called the main sequence. Stars move off the main sequence when their life starts to end. This presents a useful method for dating stellar clusters where all stars are assumed to be the same age. By plotting all the stars in the cluster in a temperature-luminosity diagram, one can simply read off the temperature of the most massive star still on the main-sequence. Since temperature is related to mass, and mass is the determining factor for the lifetime of a star, when the mass of the oldest main-sequence star is known, the age of the cluster is also known. This method for age determination is called the main sequence turn-off point.

The main sequence turn-off method works for stars in clusters or similar systems, but not for individual stars. To age individual stars, we can still use the knowledge gained by studying clusters. We can plot the line formed by stars of the same age but with different masses,

called an isochrone. Isochrones can be computed for different ages, see Fig. 2.3, and by using these, it is possible to estimate ages for single stars as well. However, the metallicity of a population will affect the shape of its isochrones, so determining the metallicity is required before an estimate of the age can be made (Bergbusch & VandenBerg 2001). Any star that leaves the main sequence is, at any given point in time, on the isochrone for that age, and if the metallicity of the star is known, the correct isochrone can be selected by fitting the current position of the star to one, and the age of the star can be determined. The weaknesses of this method are that isochrones are tightly spaced in certain regions of the temperature-luminosity space, meaning that even small errors in measurements can significantly affect the resulting age estimate, and small uncertainties in the metallicity measurement also change the set of isochrones used, which also affects the age estimates (Soderblom 2010).

If we have access to long series of high-quality photometric data for a star, we can observe its oscillations, from which several significant properties of the star can be deduced, including age. This is called asteroseismology, and the results obtained this way are usually of high quality (with errors on the order of 10%). This method can be applied to stars at any evolutionary stage, not just post-main-sequence stars (Cunha et al. 2007). Such data is available from, for example, the Kepler Asteroseismology Program (Gilliland et al. 2010), which led to the creation of, among others, the APOKASC catalogue (Pinsonneault et al. 2014), which contains asteroseismic data from Kepler and spectroscopic data from APOGEE for 1916 red giant stars. The specifics of how this method works are beyond the scope of this thesis, but ultimately, they are still dependent on a model of the star and thus share that weakness with the isochrone-fitting method. Because of the requirement for large amounts of data, this method has historically only been applied to a relatively small number of stars, but that is set to change as more and more powerful surveys come online.

In paper III we study, usually distant, populations of red giant stars, meaning the isochrone method for fitting their ages is not useful for us, and astroseismic data is not available for the vast majority of the stars. Instead, we use ages derived using machine learning as computed by Mackereth et al. (2019). Machine learning seems suited to this challenge, as determining the age of a star depends on many factors, which a neural network can take into account to estimate an answer. This works by training a model on a set of stars whose ages are known from more precise methods (e.g. asteroseismology or isochrone fitting in well-studied clusters) and having the algorithm learn the non-linear relationships between the observable spectra and stellar ages. The primary data that the model uses to make these estimations are the abundances of carbon and nitrogen, which are related to the mass of the star and therefore its age (Salaris et al. 2015). Once trained, the model can predict ages for large numbers of stars where traditional age determinations would be difficult, impractical, or impossible. For the data we use, this method has an estimated median uncertainty between 30% and 35%.

Chapter 3

The phase spiral

1 Measuring the phase spiral

The greatest discovery precipitated by the success of the *Gaia* mission was not any single object or phenomenon, but that the Galaxy as a whole was not in a state of equilibrium. Many earlier works (prior to 2017) assumed the Milky Way was more or less a steady and stable system, as discussed in Rix & Bovy (2013), a review written in anticipation of the *Gaia* mission, and numerous papers by authors such as Binney & Sanders (2016). *Gaia* revealed that this was unambiguously not the case, and the recent review by Hunt & Vasiliev (2025) goes into detail on all the discoveries in this regard. In this chapter, I will focus on one such disequilibrium feature discovered in the *Gaia* data, the phase spiral.

The phase spiral is a spiral pattern seen in stellar number density in the vertical phase plane, showing Z and V_Z on the axes. Being a fairly recent discovery, many open questions remain about the phase spiral. The most obvious one is: what caused it? The most basic explanation is simple: the Milky Way disc has an anharmonic potential, so stars moving vertically are not harmonic oscillators. Because of this, if there is any kind of perturbation to the disc that moves some stars either up or down at the same time, the stars with smaller vertical excursions will oscillate faster than those with larger excursions. This will naturally cause a spiral pattern to emerge as the stars in the inner parts of the Z - V_Z phase plane will be rotating faster than those in the outer parts (Binney & Tremaine 2008). This is illustrated in Fig. 3.1, which shows a time series of snapshots from a simple model of the potential of the disc. In it, we see the phase-space positions of stars that all start synchronised at Z=0 and moving in the same direction, upward (positive V_Z), but at different speeds. We see the stars quickly start to wind themselves into a spiral pattern as those closest to the centre of the phase space complete their round trips faster than those further out.

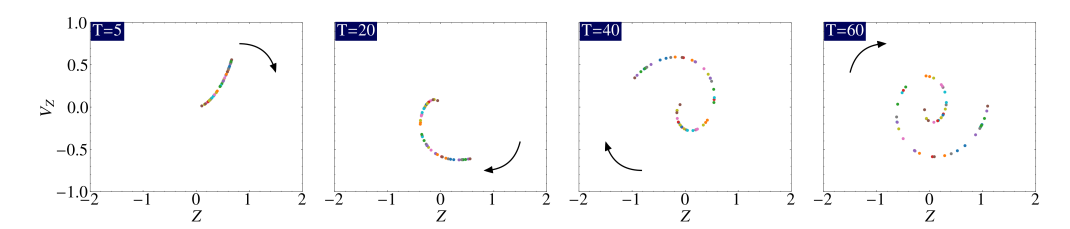


Figure 3.1: Illustration of the natural winding-up of synchronised particles in phase space, shown as a time series of snapshots of a simple model, advancing from left to right. At T=0, the stars are released from Z=0 with different, positive, Z-velocities. The stars with smaller motions (closer to the centre of the phase space) will circle faster and cause a spiral pattern to emerge over time. The arrows show the direction of motion.

One popular theory for the origin of the phase spiral is that an external object has perturbed the disc. The Sagittarius dwarf galaxy is the most often suggested candidate (Binney & Schönrich 2018; Laporte et al. 2019b; Bland-Hawthorn et al. 2019), and in that case, it was the gravitational force from the Sagittarius dwarf galaxy that acted to synchronise the vertical motions of stars in the disc. It has not been ruled out that the phase spiral is caused by some mechanism internal to the Milky Way. For instance, if the pattern speed of the Galactic bar changes, that has been shown to induce waves in the disc, causing phase spirals (Li et al. 2023). It is also likely that there are multiple causes behind the phase spiral. Hunt et al. (2022); Bennett et al. (2022) and Tremaine et al. (2023) all suggest that the formation history of the phase spiral cannot be fully explained with a single impact, but perhaps could be from several smaller disturbances. Frankel et al. (2023) and Antoja et al. (2023) both find that a simple model with a single cause for the perturbation fails to explain the observations and call for more complex models.

The first paper of this thesis investigates how the phase spiral pattern varies with location in the Galaxy. Using the early third data release from Gaia, EDR3, we grouped stars based on azimuthal position and vertical angular momentum (L_Z). We used angular momentum instead of radial distance because angular momentum dictates a star's average radial distance rather than its current distance, which produced clearer spiral patterns. This is equivalent to using the guiding centre radius in the epicycle approximation instead of the star's actual radial position. We discovered two things: the phase spiral pattern is significantly more distinct at higher angular momenta (in the 2200 kpc km s⁻¹ < L_Z < 2400 kpc km s⁻¹ range, corresponding to a guiding center radius of 9.5 kpc to 10.4 kpc), and the phase spiral has different orientations at different azimuthal angles, i.e. it appears to rotate.

The strength, or amplitude, of the spiral pattern is how distinct it is, which means what fraction of stars are participating in the spiral compared to being located randomly in phase space. The top panel in Fig. 3.2 shows how the spiral pattern looks at different angular momenta. The bottom panel shows a quantification of the strength of the phase spiral pattern

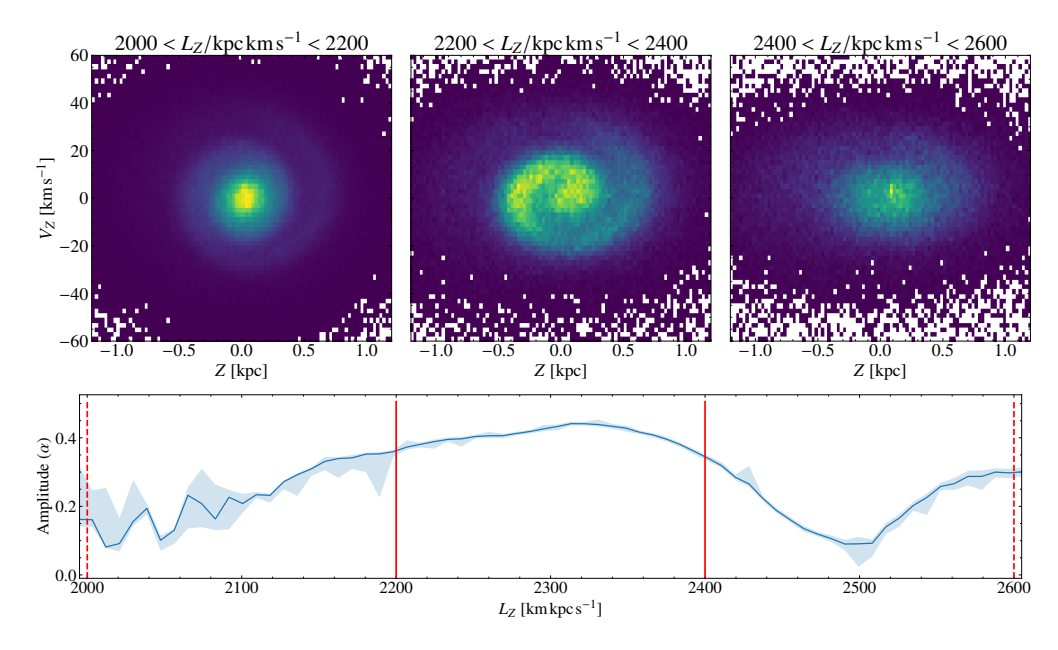


Figure 3.2: Measurements of the strength of the phase spiral as a function of angular momentum. Top: Phase spirals at 2000 kpc km s $^{-1}$ < L_Z < 2200 kpc km s $^{-1}$, 2200 kpc km s $^{-1}$ < L_Z < 2400 kpc km s $^{-1}$, and 2400 kpc km s $^{-1}$ < L_Z < 2600 kpc km s $^{-1}$. Bottom: Strength of the phase-spiral pattern as a function of angular momentum. The shaded area in the 1σ uncertainty of the fit.

Credit: Alinder et al. (2023), licenced under CC BY 4.0.

across the same range of angular momenta. We can see that the strength is significantly higher in the middle panel, between about 2200 and 2400 kpc km $\rm s^{-1}$.

We were not the first to discover the rotation of the phase spiral. It had previously been used by Widmark et al. (2022), who included the rotation of the phase spiral in their method to fit observed phase spirals, and Wang et al. (2019), who looked at the phase spiral at different Galactic azimuths when searching for changes in the amplitude of the spiral pattern. It has also been seen in simulations. Bland-Hawthorn & Tepper-García (2021) showed the rotation of the phase spiral at different Galactic azimuths in their N-body simulation of the effects of the passage of the Sagittarius dwarf galaxy on the Galactic disc, and Darragh-Ford et al. (2023) showed the rotation of the phase spiral at different Galactic azimuths and angular momenta in their model. Ours was the first study to measure, show, and explicitly discuss the rotation of the phase spiral. The rotation of the phase spiral pattern we saw is illustrated in Fig. 3.3, where a slice of the Galactic disc in azimuth (ϕ) from 210° to 150° and guiding centre equivalent radius from 8 kpc to 11 kpc is coloured by the orientation of the phase spiral found there. The zero-point of the colour scale is arbitrary, but the difference between the most and least rotated bins in a row is about π radians, or 180°.

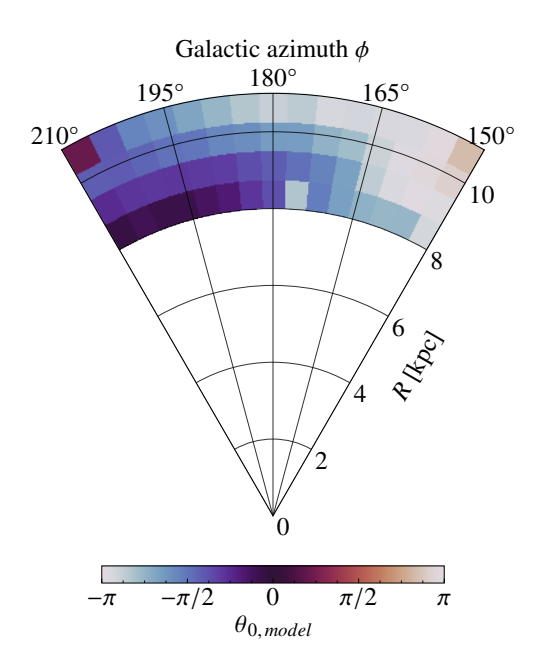


Figure 3.3: The rotation of the phase spiral measured across a range of azimuthal angles and angular momenta, shown as radius of guiding centre. The colour bar is periodic and the zero point is arbitrary.

Credit: Detail from Alinder et al. (2023), licenced under CC BY 4.0.

We also investigated whether the phase spiral shows up in the phase plane if we colour it by mean metallicity rather than number density. The result can be seen in Fig. 3.4, where the left panel (covering the 2000 kpc km s⁻¹ < L_Z < 2200 kpc km s⁻¹ range, corresponding to a guiding center radius of 8.6 kpc < R_G < 9.5 kpc) and the middle panel (2200 kpc km s⁻¹ < L_Z < 2400 kpc km s⁻¹, or 9.5 kpc < R_G < 10.4 kpc) shows a discernable spiral pattern in agreement with the spiral patterns seen in Fig. 3.2. We interpret this as the phase spiral driving high-metallicity stars from the mid-plane of the Galaxy to higher values of |Z|.

2 Quantifying the phase spiral

Figures 3.2 and 3.3 show measurements of the properties of the phase spiral. Creating a way of making these quantified measurements was one of the achievements of our first paper. The idea is to model the observed spiral pattern in phase space as a smooth background with a spiral-shaped perturbation on top. The goal is to create a mathematical model of the spiral pattern in phase space that contains the properties we want to measure from the phase spiral. Then we can adjust the parameters of our model until it matches the observations

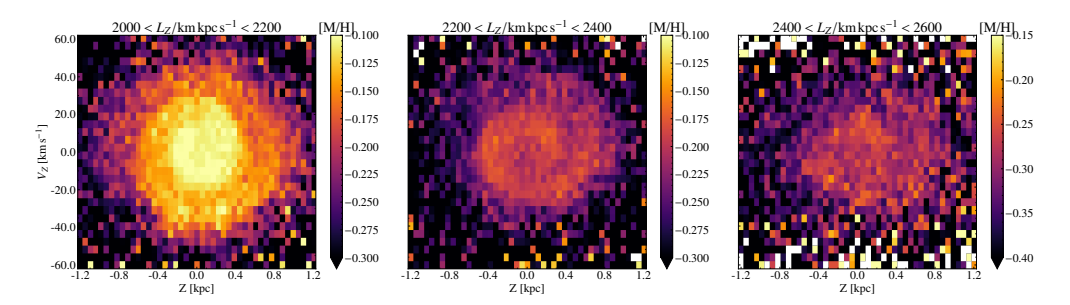


Figure 3.4: The phase plane coloured by mean metallicity at 2000 kpc km s $^{-1}$ < L_Z < 2200 kpc km s $^{-1}$, 2200 kpc km s $^{-1}$ < L_Z < 2400 kpc km s $^{-1}$, and 2400 kpc km s $^{-1}$ < L_Z < 2600 kpc km s $^{-1}$.

Credit: Alinder et al. (2023), licenced under CC BY 4.0.

and read off the parameters of the phase spiral from the model. We did this by starting with a simple quadratic spiral,

$$r = b\phi_s + c\phi_s^2. (3.1)$$

In this equation, r is the distance from the centre of phase space and ϕ_s is the rotation angle around the centre of phase space. This starting point was inspired by the discussion in Guo et al. (2022). Having both a linear term (b) and a quadratic term (c) means we can adjust the winding rate and the "acceleration" of the winding rate of the spiral. Solving Eqn. 3.1 for $\phi_s(r)$, we get

$$\phi_s(r) = -\frac{b}{2c} + \sqrt{\left(\frac{b}{2c}\right)^2 + \frac{r}{c}}.$$
(3.2)

We get the form of the perturbation from Widmark et al. (2021b),

$$f(r, \Delta\theta) = 1 + \alpha \cdot g(r)\cos(\Delta\theta), \tag{3.3}$$

where α is the amplitude of the phase spiral, g(r) is a flattening function, and $\Delta\theta$ is the phase angle defined as

$$\Delta\theta = \theta - \phi_s(r) - \theta_0, \tag{3.4}$$

where θ_0 is the angle offset, which is a free parameter, giving us

$$f(r,\theta) = 1 + \alpha \cdot g(r)\cos(\theta - \phi_s(r) - \theta_0). \tag{3.5}$$

In this formulation, 1 is the (normalised) background and $\alpha \cdot g(r) \cos(\theta - \phi_s(r) - \theta_0)$ is the perturbation of the background. α takes values between 0 and 1. If $\alpha = 0$, the perturbation term vanishes, the background is left unperturbed, and the phase spiral does not exist. If $\alpha = 1$, the phase spiral dominates over the background and the phase-space density away from the spiral (between the windings of the spiral arm) falls to zero.

The flattening function g(r) takes the central parts of phase space and "flattens" them, i.e. it reduces the strength of the perturbation. We need to reduce the importance of the central region to make our model fit the data well, and that is done with this function. We do this because our model defines the phase spiral in full detail, even to very low distances from the centre of phase space. Stars in this region are almost at rest in the Z-direction, so our data always shows more or less of a clump or blob in this central region. The flattening function takes the form

$$g(r) = \text{sigm}\left(\frac{r-\rho}{0.1 \text{ kpc}}\right),$$
 (3.6)

where

$$sigm(x) = \frac{1}{1 + e^{-x}},$$
(3.7)

is the sigmoid function and ρ is the radius parameter of the function.

Finally, we also want to reduce the influence of the corners of the plots, the most distant regions of the phase plane, where there are very few stars. In the upper row of Fig. 3.2, we see white pixels in the corners, which means there are no stars there. Again, following the lead of Widmark et al. (2021b), we multiply both data and model by a term that we call mask. We define it as

$$mask(Z, V_Z) = -sigm\left(\left(\frac{Z}{1 \, \text{kpc}}\right)^2 + \left(\frac{V_Z}{40 \, \text{km s}^{-1}}\right)^2 - 1\right) - 1.$$
(3.8)

We apply this mask because the outermost regions of phase space are very sparse and therefore will only contribute noise to the fitting evaluation.

With all this done, we can combine Eqs. 3.2, 3.5, and 3.6, which gives us the spiral perturbation as

$$f(r,\theta) = 1 + \alpha \cdot \text{sigm}\left(\frac{r-\rho}{0.1 \text{ kpc}}\right) \cos(\theta - \phi_s(r) - \theta_0), \tag{3.9}$$

where α , ρ , and θ_0 , as well as b and c, are the parameters of the model that can be adjusted. Fitting the model to the data is done in several steps. Figure 3.5 shows the steps and serves as a visual aid.

- 1. Create the 2D histogram of the phase spiral using data (panel a).
- 2. A guess at what the background could be is created by blurring and mirroring the data (panel b).
- 3. Use a Markov chain Monte Carlo algorithm approach to fit a perturbation multiplied by the background to the data (panel d).

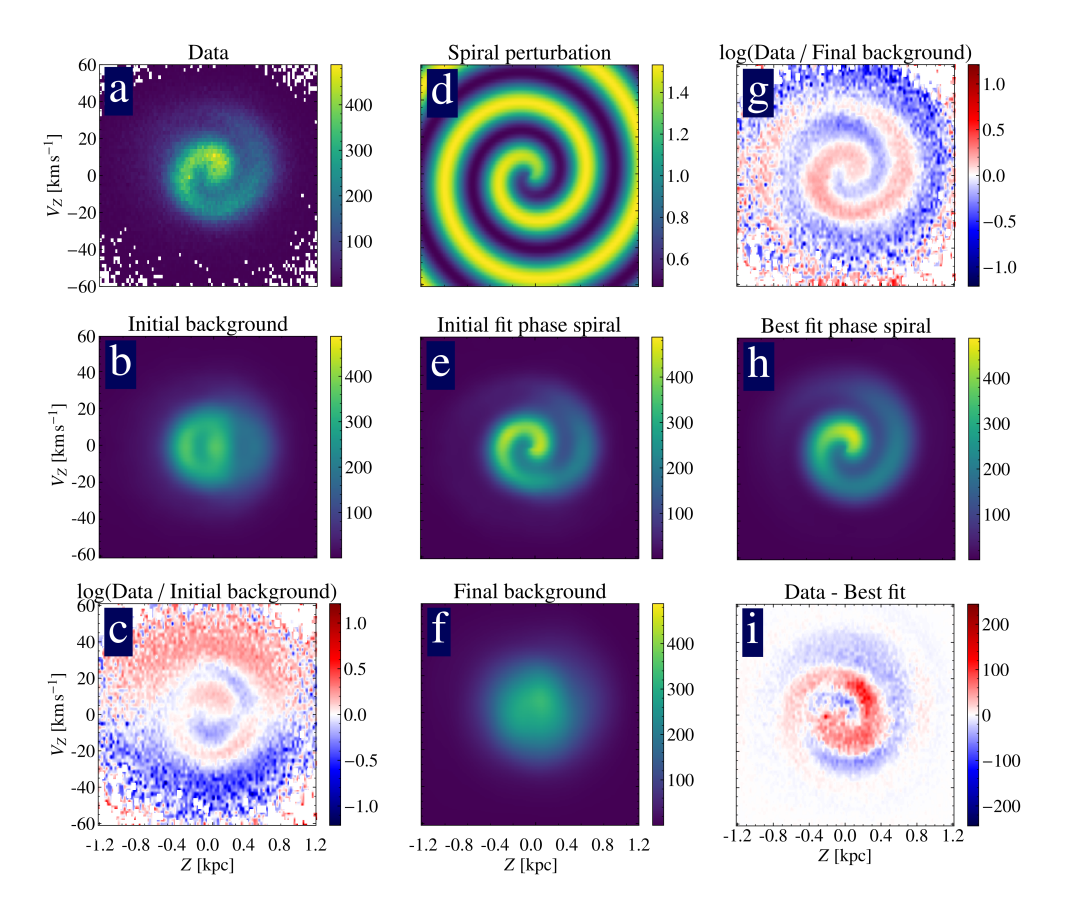


Figure 3.5: Example process for fitting our model to data. a: Data used for the model, a two-dimensional histogram showing the number density of stars, b: Initial background, c: Data divided by the initial background, d: Extracted spiral perturbation, e: Initial fit spiral. f: Final background after iterative refinement, g: Data divided by the final background, h: Best fit spiral. i: Residuals as computed by Data (panel a) — Best fit (panel h).

Credit: Reproduced from Alinder et al. (2023), licenced under CC BY 4.0.

- 4. This will inevitably be an imperfect fit (panels c & e). By dividing the data by the spiral perturbation, we create a new background (panel f) and repeat the procedure from step 3. This is repeated until the new background no longer provides a significant improvement over the old one. This will break the symmetry of the background introduced in step 2, which is good since the real background does not have to be symmetric (compare panels c and g).
- 5. The result of the procedure is a spiral with a good fit (panel h) from which the parameters of the phase spiral in the data can be read off. Subtracting the data from the bet fit spiral reveals a good match with the most notable difference being an

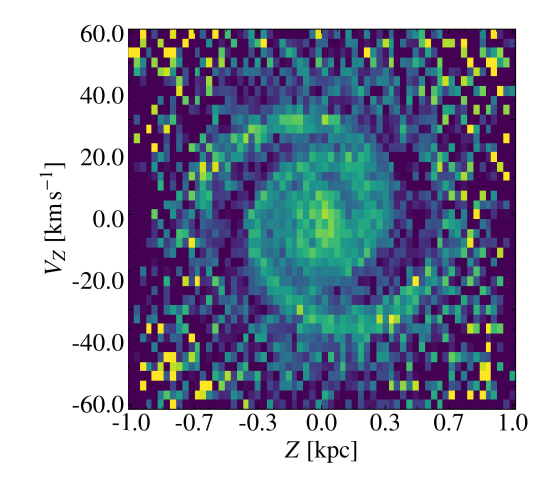


Figure 3.6: The two-armed phase spiral in the solar neighbourhood, enhanced with kernel density contrast to increase viability.

Credit: Detail from Alinder et al. (2024), licenced under CC BY 4.0.

underestimation of the number of stars in the trough away from the spiral (panel i).

This method has the advantage that it is independent of assumptions about the mechanism causing the phase spiral and models of the Galaxy. It is efficient, usually converging on a solution after three iterations, and works well even when given sparse data, making it suitable for mapping phase spirals far from the Sun.

3 The two-armed phase spiral

The story of the phase spiral gained a significant wrinkle when Hunt et al. (2022) discovered another phase spiral pattern. When investigating stars in the solar neighbourhood with low angular momentum, meaning they are on eccentric orbits and currently near their outermost point, a phase spiral with two arms, like in Fig. 3.6, appeared in the data. Our second paper was about exploring the properties of this phenomenon.

We modified the model fitting procedure described above to use two perturbations, two independent spirals, instead of one. It is still unknown whether the two-armed phase spiral is a genuine two-armed spiral or two one-armed spirals that overlap. We chose to use two independent spirals because we did not want to assume one scenario over the other, but allow for both. By modelling two separate one-armed spirals, if the data contains a single two-armed spiral, the results should reflect that behaviour by having the two arms always be opposite each other. The distinction between a two-armed spiral and two one-armed

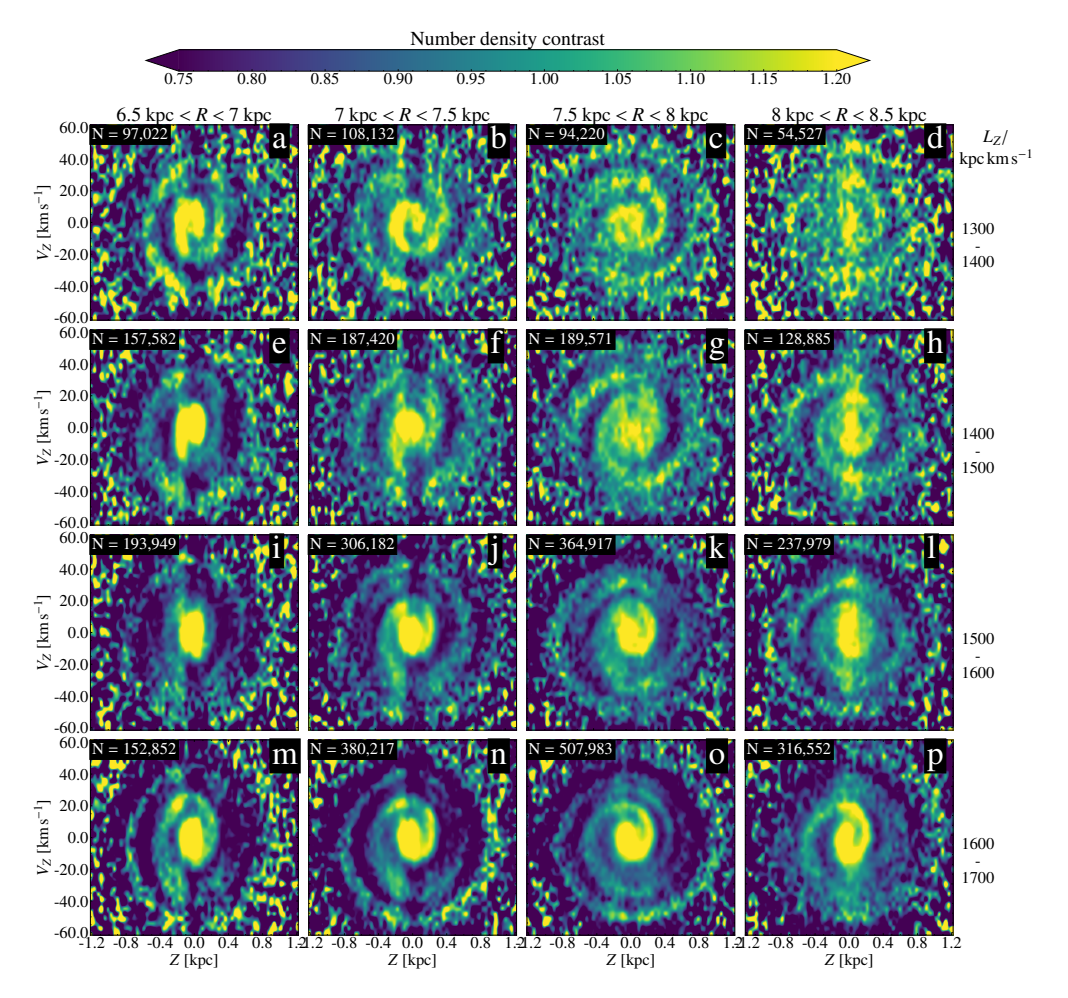


Figure 3.7: Density contrast in the Z - V_Z phase plane at different radii and angular momenta, showing the one- or two-armed phase spiral. The rows have different angular momenta, shown on the right, and the columns have different radial distances, shown on top. The number in each panel displays the number of stars included.

Credit: Alinder et al. (2024), licenced under CC BY 4.0.

spirals lies in the mechanism that created or maintains the spiral pattern. In the case of a two-armed spiral, the spiral pattern is created when something displaces different groups of stars upwards and downwards at the same time. This is known as a "breathing mode" from how the disc would appear to oscillate between being more and less vertically extended over time in simulations. Breathing modes can be produced by interactions with an external perturber, and are more likely to happen if the encounter is fast (Widrow et al. 2014), or they can arise without any external perturber (Hunt et al. 2022). The mechanism for producing two one-armed spirals would conceivably be the same as the one that pro-

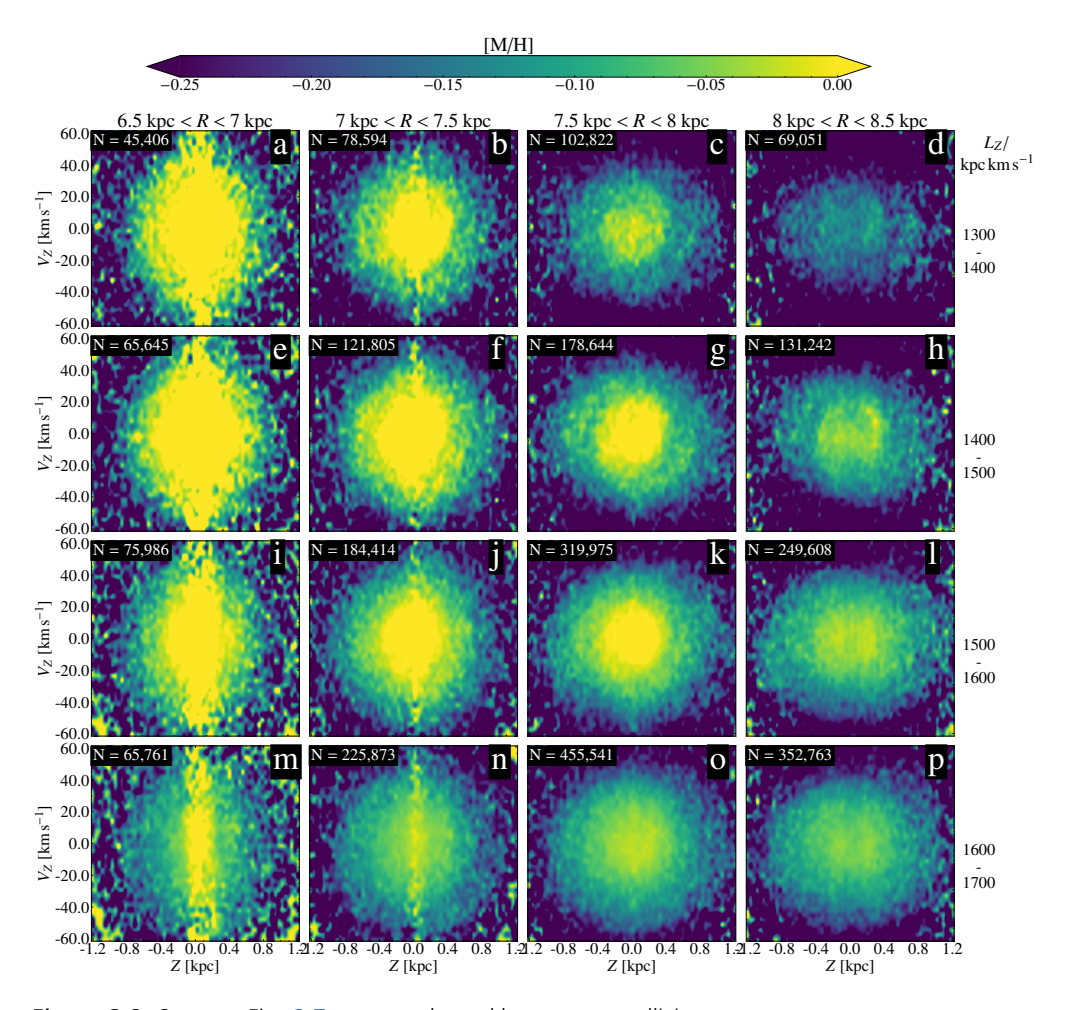


Figure 3.8: Same as Fig. 3.7 except coloured by mean metallicity. Credit: Alinder et al. (2024), licenced under CC BY 4.0.

duced the single one-armed spiral, simply repeated. For example, if there were two dwarf galaxies that perturbed the Milky Way disc, that could produce two one-armed phase spirals. However, no suitable objects have been observed that could have caused this to happen to the Milky Way.

Our intention with our second paper was to measure the properties of the two-armed phase spiral in much the same way as we had done with the one-armed spiral in paper I. The two-armed phase spiral pattern is weak, so we needed to use so-called kernel density contrast to enhance our plots. This means creating a much-blurred version of the image by using a Gaussian filter and subtracting it from the original image, thus enhancing any non-smooth features.

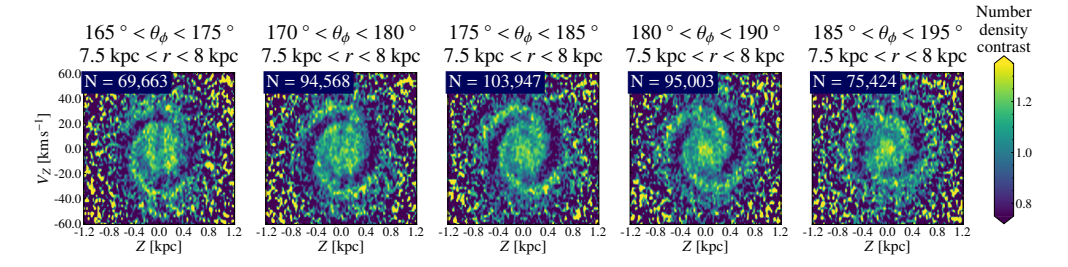


Figure 3.9: Number density contrast in the phase plane showing the two-armed phase spiral at different phase angles (θ_{ϕ}) , which shows the rotation. The phase angle increases from left to right.

Credit: Alinder et al. (2024), licenced under CC BY 4.0.

The first thing we investigated was where the two-armed phase spiral could be found. Previously, it had only been detected in the solar neighbourhood at low angular momentum, approximately 1500 kpc km s⁻¹ or $R_G \approx 6.3$ kpc. We selected stars in a grid of different angular momenta and Galactocentric radial distances to search for phase spirals, shown in Fig. 3.7. These results showed that the two-armed phase spiral could not be found anywhere except where it had already been previously seen. Unexpectedly, this was not a structure that could be seen at low angular momenta, just in the specific 1400-1500 kpc km s⁻¹ range and close to the Sun (panel g). We also investigated if the radial position of the stars had an effect and found that most of the two-armed spiral pattern remains if we move the selection 500 pc radially out but keep the same angular momentum cuts (panel h). Since the Galactocentric radial distance of the Sun is taken to be 8.122 kpc in Paper II, both panel g and h can reasonably be claimed to contain the solar neighbourhood.

We also investigated the spiral pattern in mean metallicity for the two-armed phase spiral in the same way as for the one-armed one, by colouring the phase place with mean metallicity instead of stellar number density, or density contrast in this case. The results are shown in Fig. 3.8, where, in panel g, we barely see a pair of ridges of slightly higher metallicity in the locations where the spiral pattern is seen in Fig. 3.7.

Next, we investigated whether the two-armed phase spiral rotates within the range of angular momentum where it was detected. We were able to confirm that it, like the one-armed version, has different rotation angles across the Galactic disc, as is shown in Fig. 3.9. We used phase angle instead of azimuthal angle because it produces a clearer pattern, much like angular momentum, compared to radial position and for the same reason, the phase spiral is a dynamic structure where the history of the stars matters and dynamic selection criteria, like angular momentum and phase angle, capture this much better. Because we changed our selection to use phase angle, we also recreated the results from paper I using this technique to verify that it produced the same results. We found that it did, the "normal" one-armed phase spiral looks and acts the same regardless of whether azimuthal angle

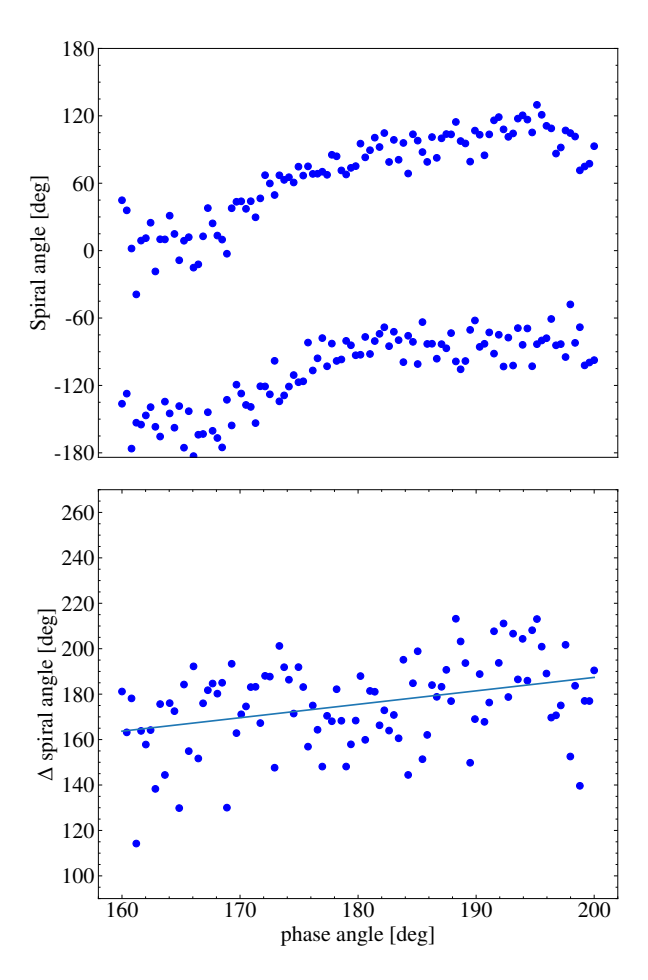


Figure 3.10: Measurement of rotation of phase spirals at different phase angles. Top panel: phase spiral rotation angles as functions of phase angle. Each phase spiral forms its own track. The data is from the solar neighbourhood (d < 1 kpc), and each point covers data from $\pm 3.5^{\circ}$. The zero point of the spiral angle is arbitrary. Bottom panel: difference in the rotation of the phase spirals. The trend is fitted with a line. Credit: Alinder et al. (2024), licenced under CC BY 4.0.

or phase angle is used to select the stars. The spiral pattern is strong enough that the extra clarity provided by the selection using phase angle is barely perceptible.

We plotted the rotation of the spirals against position in the disc as measured by the phase angle in Fig. 3.10. Since we used two independent one-armed spirals in our model, our results show as two tracks in the figure, one for each spiral arm. With these independent measurements, we can compare the angles of the spiral arms against each other. In the bottom panel of Fig. 3.10, we plotted the difference in angle between the spiral arms and fit the trend with a straight line. It seems the angle between the spiral arms is increasing

slightly with phase angle.

Chapter 4

Scale-heights of the Milky Way discs

When doing research on the structure of the Galaxy, the ability to categorise stars based on which component they belong to is often required. A study of thick disc stars needs a way to select a sample of thick disc stars, for example. This is complicated by the fact that the Milky Way, like most galaxies, contains a mix of different stellar populations whose properties sometimes overlap. Different studies tend to use different criteria for doing this categorisation, depending on what data they have available and which science questions they want to answer, and there are several methods to choose from. Based on which data they use, I would organise these methods as:

- Geometric, where the position of a star within the Galaxy is used to categorise it. A star that is close to the plane of the disc is a thin disc star, and one that is far from the plane is a thick disc star.
- Chemical, where the composition of a star is used. The most common abundances to use are $[\alpha/\text{Fe}]$ and [Fe/H], in which two sequences of stars can be observed. The high- α sequence is identified with the thick disc, and the low- α sequence is identified with the thin disc (Bensby et al. 2011; Bovy et al. 2012; Cheng et al. 2012).
- Kinematic, where the motion of a star is used. Thick disc stars have larger velocity dispersions, and in general less flat and circular orbits than thin disc stars (Binney & Merrifield 1998).
- Dynamical, where the further orbital properties of stars are taken into account for categorisation. This allows quantities such as orbital actions or energy to be used, which can provide information about past associations (Binney & Tremaine 2008).
- Chronological, where the ages of stars are used. If the thick disc formed before the thin disc, then the ages of stars should be a way to categorise them.

With such a variety of methods to choose from, it is important to know how your choice of definition can affect your results. In our third paper, we compare several methods for categorising stars as belonging to the thick disc or thin disc. We used data from APOGEE DR17 (Abdurro'uf et al. 2022) with careful cuts to get a high-quality sample that was also representative of the Galactic population. We used the selections produced by the different methods to construct models of the vertical density of the Milky Way to evaluate them and compare them against each other.

1 Disc model

The model we used for comparing the results of the selections we tested consisted of two exponential discs with vertical densities in the form

$$N(Z) = \exp\left(-\frac{|Z|}{H}\right),\tag{4.1}$$

where *H* is the scale height of the disc, the distance over which the density of the disc decreases by a factor of *e*. Two instances of this disc model (one for the thin disc and one for the thick disc) were combined with a simple constant term for the halo to create our model,

$$N_{\text{total}}(Z) = f_d \times N_1(Z) + (1 - f_d) \times N_2(Z) + C_{halo}, \tag{4.2}$$

where f_d is the thick disc fraction in the plane. We fit the model to our data by matching the fractions of each structural component, as measured by the methods listed below, across a range of heights in radial bins from 3 kpc to 15 kpc. Because we always consider relatively small volumes of the Galaxy at a time, we can approximate the halo as a constant. This means we do not need to select and fit a halo model in addition to the disc models, which simplifies the process and removes a potential source of errors.

We used a Markov-Chain Monte-Carlo (MCMC) method again to find the most likely model to fit the data, using the emcee (Foreman-Mackey et al. 2013) package, which applies the Goodman-Weare algorithm (Goodman & Weare 2010).

2 Selection methods

2.1 The abundance methods

The chemical composition of a star can tell us about the environment where that star formed. We focus primarily on the abundances of two elements here, Mg and Al. As explained in Chapter 1, α -elements like Mg are produced earlier in the process of galactic

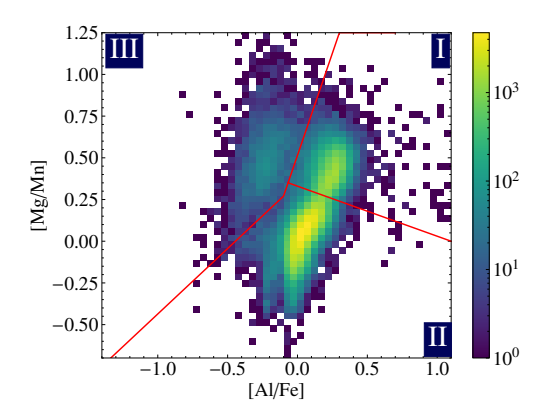


Figure 4.1: Stellar number density in the [Mg/Mn] - [Al/Fe] plane with the selection into disc components shown with red lines. Region I is the thick disc, Region II is the thin disc, and Region III is the accreted or non-disc stars.

chemical evolution and alpha abundances ([α /Fe]) can therefore serve as crude chronometers. The production rate of Al is correlated with mass and metallicity, with means more massive and metal-rich stars produce more Al (Nordlander & Lind 2017). Because of this, smaller systems like dwarf galaxies will have lower [Al/Fe] in their interstellar medium and in their stars than larger systems like the Milky Way.

This is the basis for the two chemically based methods we tested. The first one uses a cut in the [Mg/Mn] - [Al/Fe] plane to take advantage of the properties of both Al and Mg (Hawkins et al. 2015; Das et al. 2020). In this plane, the thick and thin discs are two dense areas on a sequence along [Mg/Mn] that only changes slightly in [Al/Fe], and the halo and accreted stars are separated in a parallel sequence, see Fig. 4.1. This allows us to make a clear cut to separate non-disc stars, and the disc components are separated through the least dense area between them. The second method uses a cut in the [Mg/Fe] - [Fe/H] plane, in which the separation between the disc components is relatively clear (Fuhrmann 1998), shown in Fig. 4.2. The halo and accreted stars are harder to separate than in the [Mg/Mn] - [Al/Fe], so a simple cut-off in [Mg/Fe] is used.

These methods work well with the only downside being that it is fairly costly or labour-intensive to acquire sufficiently high-quality data to measure the abundances for a large number of stars, thus limiting sample size. Several large-scale projects to gather more data will soon come online and potentially change this.

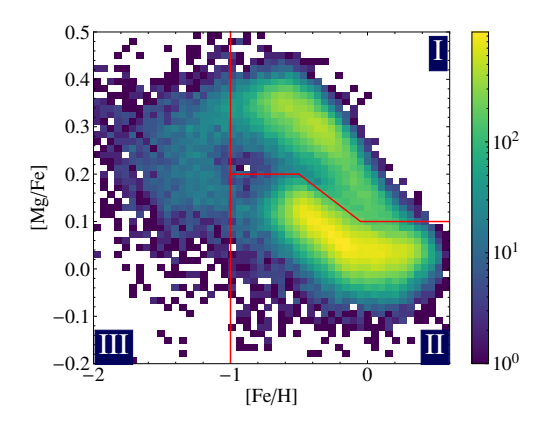


Figure 4.2: Stellar number density in the [Mg/Fe] - [Fe/H] plane with the selection into disc components shown with red lines. Region I is the thick disc, Region II is the thin disc, and Region III is the accreted or halo stars.

2.2 The kinematic and dynamical methods

With the success of the *Gaia* mission, we have an abundance of positional and kinematic data. A reliable method using this kind of information, rather than abundances, would provide access to a large amount of data that astronomers could use to study the components of the Galaxy.

Compared to the methods using abundance data, methods using kinematic data have a large drawback. Kinematic information is not well preserved over time, and distinct populations of stars can blend together. Purely kinematic methods have been used in the past to successfully separate the discs (e.g. Bensby et al. 2005), but suffer from the drawback that they need accurate velocity dispersions to work. Velocity dispersions are possible to compute, but become labour-intensive for areas far removed from the Sun. These methods use the empirical kinematic properties of the discs. In the plane, thick disc stars not only have larger vertical velocities, but they also seem to orbit slower on average than thin disc stars. This is called asymmetric drift. The reason for this drift is that thick disc stars have more eccentric orbits on average, and a star on an eccentric orbit will spend most of its time moving slowly in the outer part of its orbit, so when observing the stars around us, we measure the average azimuthal velocity of thick disc stars to be lower. We test a method using kinematic properties, but due to the restrictions on it, we only apply it in a region relatively close to the Sun.

In an attempt to use more powerful tools to bypass the issues with the purely kinematic selection, one of the methods we test uses action-angle coordinates as the basis for selection. Actions are integrals of motion and, as such, they stay constant for a star over time. We generally define three actions. The radial action (J_R) , which indicates radial oscillations or

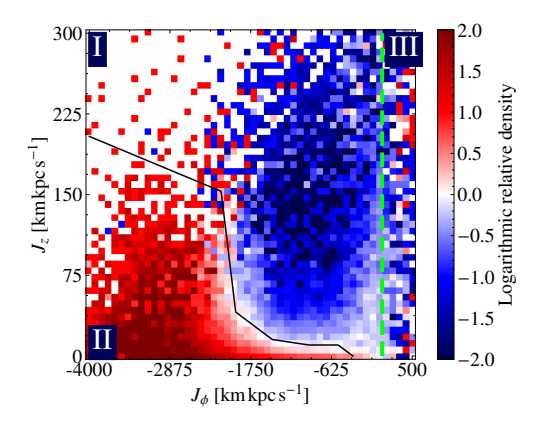


Figure 4.3: Relative stellar number density of the disc components in the J_{ϕ} - J_{Z} plane. The separation of the disc components is shown with a black line, and the region of accreted or halo stars is marked with a dashed green line. Region I is the thick disc, Region II is the thin disc, and Region III is the accreted or halo stars.

orbital eccentricity, the vertical action (J_Z) , which indicates vertical oscillations, and the azimuthal action (J_ϕ) , which is the same as vertical angular momentum (L_Z) . The angles are the conjugate coordinates of the actions and describe the phase of the star on its orbit (Binney & Tremaine 2008). They are simplest to understand in terms of the guiding centre and epicycle approximation discussed in Chapter 2. They are the radial angle (θ_R) , which is the phase of the star in its radial oscillation around the guiding centre and takes values 0 at pericentre and π at apocentre, the vertical angle (θ_Z) , which is the phase of the star in its vertical motion about the Galactic mid-plane and takes values 0 in the plane and $\pm \frac{\pi}{2}$ furthest above or below, and the azimuthal angle (θ_ϕ) , which is the angular position of the guiding centre around the Galaxy.

Actions are convenient to work with because they are constant over time. The radial position of a star will be constantly changing unless it is on a perfectly circular orbit, but the radial action describes how much the star moves in the radial direction, which is constant over time. Actions have a further advantage over simpler measures like eccentricity, which only measures the radial motion for the current orbit, in that they remain constant even in a changing potential, assuming the change is slow compared to the period of the orbit. This kind of change is called adiabatic, and the actions are therefore called adiabatic invariants.

For our studies, we used AGAMA by Vasiliev (2019) with a potential from McMillan (2017) to compute actions for our stars when needed. To compute actions and angles, the potential needs to be separable. A common solution to this, and the one we used, is to use the so-called Stäckel fudge. This involves approximating the potential of the Galaxy as a Stäckel potential, which has the favourable property of having a separable equation, meaning it is easy to derive the integrals of motion required for the actions (Binney 2012).

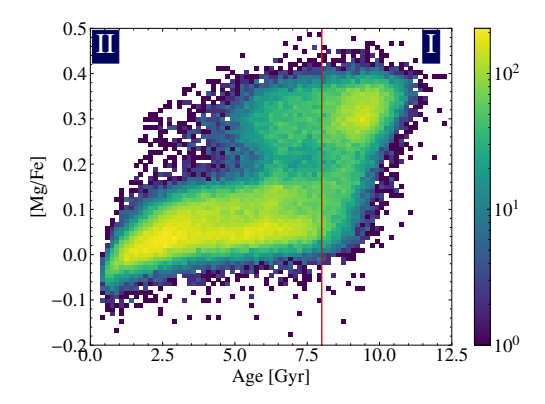


Figure 4.4: Stellar number density in the age vs [Mg/Fe] plane. 8 Gyr is marked by a red line. Area I is the thick disc, Area II is the thin disc.

In our study, we wanted to find which regions in the J_{ϕ} - J_{Z} plane correspond to which Galactic component. Intuitively, thin disc stars should occupy a region with low J_{Z} and low J_{ϕ} since they have low vertical excursions in the inner parts of the Galaxy, but flare out to occupy a region with higher J_{Z} at higher J_{ϕ} in the outer Galaxy. We decided to use the definition from the [Mg/Fe] - [Fe/H] method to initially identify the populations in J_{ϕ} - J_{Z} as thin or thick disc and to colour the space according to their relative densities, shown in Fig. 4.3. Then we used the region of equal density as the dividing line between the populations. A downside of this method is that it can only classify a region as having exclusively thin disc stars or exclusively thick disc stars, while the regions in reality can be quite mixed.

2.3 The chronological method

Even though the exact origin of the thick disc is unknown, the general consensus is that it is, at least on average, older than the thin disc, most often seen in its higher α -abundance Bensby et al. (2003). If direct age measurements could be made, it would be a very powerful tool for categorising stars. Unfortunately, such direct measurements do not exist, except for rare exceptions, so for our investigation, we used estimates of ages derived by ASTRONN, which is a neural network by Leung & Bovy (2019). The data we used uses the spectra from APOGEE DR17 as input to the neural network to determine many different parameters of the stars, such as abundances, distances, and ages, by training against known results. This lets it estimate ages for a large fraction of the APOGEE catalogue (Mackereth et al. 2019).

To visualise the distribution of ages of stars, we show Fig. 4.4, which shows magnesium abundance against age. We see a continuous dense region of stars that go from 0 to almost 10 Gyr and stays below [Mg/Fe] = 0.2, this matches the low- α thin disc, and another dense

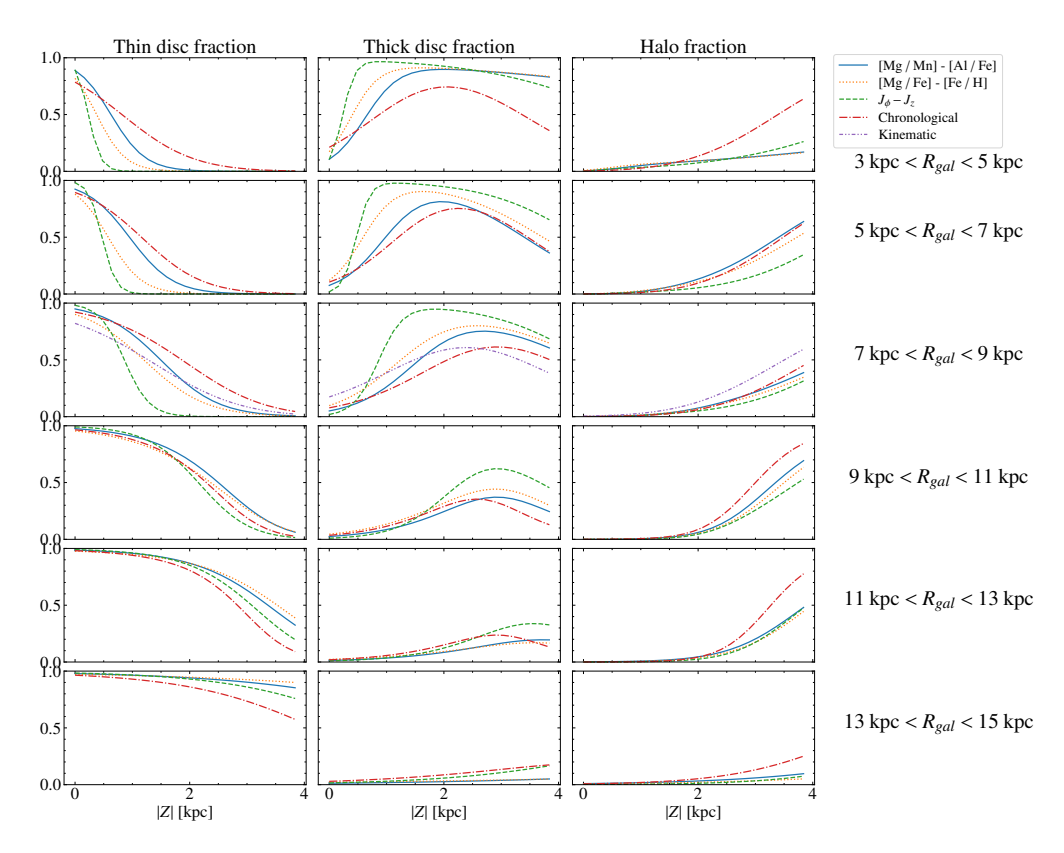


Figure 4.5: The fitted models (parameters derived with MCMC) of the relative fraction of each major component based on the methods presented above and in paper III, shown as coloured lines. From top to bottom, bins of increasing Galactocentric radial distance are shown. The methods are shown as lines of different colours and styles: the Chemical selection using a line in the [Mg/Mn] - [Al/Fe] plane is a solid blue line, the Chemical selection using a line in the [Mg/Fe] - [Fe/H] plane is a dotted orange line, the Dynamical selection is a dashed green line, the Chronological selection is a dash dotted red line, and the Kinematic selection is a dash double-dotted purple line that is only present on the $7 > \text{kpc } R_{gal} > 9 \text{ kpc row}.$

region above [Mg/Fe] = 0.2 with ages between approximately 3 and 11 Gyr, though the young end is very diffuse, which matches the high- α thick disc. This fuzziness of the young end of the thick disc is noteworthy, as this is younger than thick disc stars are expected to be. Apart from scatter for error in the age estimation, this population could be blue stragglers. These are stars that look younger than they are because they have interacted with other stars during their lifetimes. They are thought to be the result of either mass transfer from one star to another or two stars that merged. Either way, the result is a star that looks much younger than it is (Haywood et al. 2013; Cerqui et al. 2023).

To separate the stars into thin and thick discs using age, we simply divide the sample into

two at a specific point. We chose 8 Gyr for this threshold age because Jurić et al. (2008); Bensby et al. (2014) and Martig et al. (2016), among others, indicate that this is approximately the time when the thin disc started to form, so a selection of 8 Gyr or older should include a majority of the stars in the thick disc. This resulted in a relatively good selection that has the downside that it is difficult to select halo or accreted stars using it. The stars we want to separate, halo and accreted stars, can be expected to have ages between 8 and 13 Gyrs (Das et al. 2020), which overlaps with the thick disc. To select such stars, we instead use parts of the [Mg/Fe] - [Fe/H] method, and use [Fe/H] < -1 as the criterion for inclusion in this population. The biggest problem with this method is that there is less data available for use with it, as accurate age estimations are difficult to obtain, and data with low errors is an even smaller subset of that. Hopefully, this will change in the foreseeable future with large spectroscopic surveys like 4MIDABLE coming online (Bensby et al. 2019; Chiappini et al. 2019).

3 Scale parameters

We use the methods described above to fit our model and find that all methods agree on the large-scale features of the discs, but differ in the details. Figure 4.5 shows the fractions for the Galactic components as derived by the model for each categorisation method for a range of radial bins. All methods show similar general trends: the thin disc is short in the inner disc but becomes more dominant further out, the thick disc becomes weaker with Galactocentric radius and is almost completely missing in the outermost radial bins, and the fraction of thick disc stars in the plane goes down with radius. While these results are not in complete agreement with each other, the general trends agree with expectations from the literature (e.g. Bensby et al. 2011; Yoshii 2013; Katz et al. 2021).

Figure 4.6 shows the model parameters for the categorisation methods as functions of radial distance. The thick disc scale height has relatively large uncertainties but shows a decreasing trend until a Galactocentric radial distance (R_{gal}) of 10 kpc, with the different models converging to a value of about 1 kpc. The scale heights and their scatter increase again at $R_{gal} > 10$ kpc, especially in the last bin. At this distance, the overall density of the thick disc is very low, as we can see in the bottom two rows of Fig. 4.5, so the scale heights are less meaningful. A disc that goes from a very low value to essentially zero can do so very slowly, with a large scale height, but still be a minor component in that region. The fraction of thick disc stars in the plane (the Disc Ratio) decreases exponentially with increasing radial distance, reaching a minimum of about 2% in the outer disc. The thin disc scale heights increase with R_{gal} for all models except one, showing an exponential increase from approximately 200 pc to between 1 kpc and 2 kpc. That exception is the chronological method, and it shows a thin disc scale height that stays at approximately 500 pc until it increases to about 1 kpc at the same distance as the other methods.

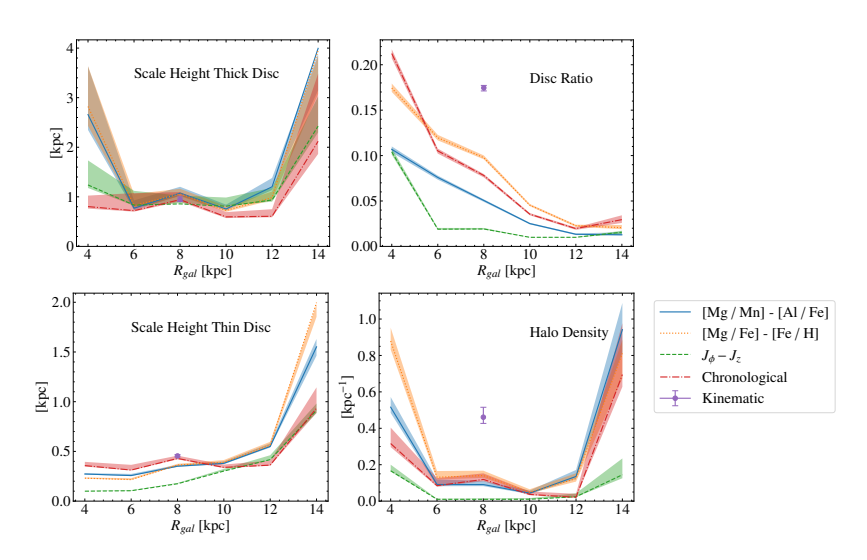


Figure 4.6: Values of the model parameters for different selection methods across a range of radial distances. Top row: The scale height of the thick disc and the fraction of thick disc stars in the Galactic mid-plane. Bottom row: The scale height of the thin disc, and the density of the halo. The shaded region is the 1σ uncertainties of the model fit.

Chapter 5

Discussion and Outlook

1 Paper I

The research into the *Gaia* phase spiral has only been ongoing for a relatively short time, but has had a noticeable impact on the fields of Galactic archaeology and Galactic dynamics. Widmark et al. (2021a,b) used it to infer the potential of the Milky Way disc, Bland-Hawthorn & Tepper-García (2021) used a simulation of the creation of phase spirals by an interaction with the Sagittarius dwarf galaxy to estimate the mass history of the dwarf galaxy, and Laporte et al. (2019b) used a simulation of the creation of phase spirals by an interaction with the Sagittarius dwarf galaxy to estimate the time of last pericenter for the Sagittarius dwarf galaxy, to mention only a few. These studies demonstrate how the phase spiral is relevant to the broader understanding of the structure and history of the Milky Way.

Our own work has focused on understanding the Milky Way from an observational perspective. We learned that the phase spiral's orientation changes with azimuth, which makes it look like a wave propagating along the disc, and that the strength of the spiral pattern increases at higher vertical angular momentum, or equivalently, toward larger guiding-centre radius. This stronger spiral pattern seen in the outer disc can be explained by the decreased potential in this region. In a very simplistic view, an external mass pulling on the Milky Way will exert the same force on stars in different regions, but stars in the outer disc feel a weaker restoring force from the Galactic disc and are therefore displaced more. Patterns in phase space are also expected to persist and be clearer for longer in the outer disc because of both the lower gravitational potential, meaning structures evolve more slowly, and diffusion in phase space, caused by interactions with other bodies in the disc, like giant molecular clouds, causing small perturbations of the structure, are rarer since the disc is more diffuse

(Laporte et al. 2022). These empirical constraints on the phase spiral can serve as boundary conditions for theory, which is our hope for the future. Any viable model, whether invoking an external perturber, secular changes in the pattern speed of the central bar, or some other mechanism, must be able to explain the observed phenomena in order to be able to claim to have found a full explanation.

2 Paper II

The two-armed phase spiral adds an interesting complication to the study of the phase spiral, because we only detect this pattern in a narrow range of vertical angular momentum. This is a significant difference from the one-armed phase spiral, which is found throughout the disc. This difference hints at a difference in mechanism or origin. But, like the one-armed phase spiral, we detected that its rotational angle varies with the phase angle selection, again like a wave propagating along the disc.

The two-armed phase spiral has been interpreted in two main ways. One view holds that it is a single spiral structure with two arms. This is described as having wavenumber m=2, because a factor is 2 is added to the sinusoidal function describing the density of the spiral perturbation as a function of phase angle (Widrow et al. 2014). This makes it a vertically symmetric "breathing" oscillation that naturally imprints a two-armed pattern in the (Z, V_Z) plane. This form of oscillation is called a breathing mode because stars are moving up and down at the same time, making the disc look as if it is pulsating. The other kind of oscillation is when stars are moving coherently in only one direction, called a bending mode. Theory predicts a correspondence between breathing modes and two-armed spirals, while bending modes produce one-armed spirals (Widrow 2023). Phase spirals with m=2 are associated with internal, in-plane perturbations such as the Galactic bar and spiral structure, possibly appearing near resonances in the inner disc (Hunt et al. 2022). Another option is that the two arms are not a single m=2 structure but rather a superposition of two distinct one-armed m=1 spirals, each started by a different perturbation. It is possible to model such structures and recover a two-armed pattern without invoking a genuine m=2 mode (Lin et al. 2025). This scenario requires multiple objects to perturb the disc, but no good candidate objects that would have caused two perturbations with the required timings have been observed.

Our model for quantifying the two-armed phase spiral used two independent one-armed phase spirals so as not to make an *a priori* assumption of an m=2 spiral. This allowed us to measure the relative angle of the spiral arms for a range of phase angles. Under the assumption that the phase spiral is not being driven by some mechanism, the only thing affecting the rate of rotation is the potential of the disc at that location. We observed a slight increase in the difference in angle between the two spiral arms across the observed range of

phase angles. If the two spiral arms are the result of two sequential external perturbations, those same perturbations might have affected the matter in the disc enough to, locally and temporarily, change the potential and therefore the rotation rate of the spiral. One needs to keep in mind that we are not looking at a time series regarding this rotation, but different current positions in phase space. It is thus possible that the second impact has disrupted the first phase spiral enough to not make it rotate the same across space but not enough to erase it completely, as is discussed in Lin et al. (2025). It is also possible that the change in relative angle we measured is due to uncertainties in our data and model, and not a physical effect.

3 Paper III

We compared several techniques to assign stars to the thick or thin disc and then evaluated how the effects of those choices propagate into the inferred parameters of those discs. Selections based on chemical abundances, using either [Mg/Mn] and [Al/Fe] or [Mg/Fe] and [Fe/H], give similar results and produce relatively clean separations of disc components. In our implementation, the [Mg/Mn] - [Al/Fe] method produced a thinner thick disc and a thicker thin disc than the [Mg/Fe] - [Fe/H] method because its definition of thin disc includes stars that the [Mg/Fe] - [Fe/H] method classifies as thick disc, due to there not being a clear break between the disc components in the [Mg/Mn] - [Al/Fe] plane. The age-based selection, using data derived through machine learning, finds a thin disc scale height that is constant along the disc until it flares in the outer disc. It has the issue that the oldest parts of the thin disc and the youngest parts of the thick disc overlap, which makes a clean selection purely based on age difficult, and it currently has to operate on a smaller dataset because accurate ages are not available for all stars. The dynamical selection in action space works with populations that are strongly blended, making categorisation difficult. Because any region in the J_{ϕ} - J_{Z} plane can only contain one type of star, this method finds the thick disc fraction in the plane to be its minimal value for all radial bins except the innermost one. We only apply the kinematic method to the radial bin that includes the solar neighbourhood because this is the only region where the method is valid. It encounters the same mixed populations as the dynamical method, but is designed to make a probabilistic statistical selection. It finds values for the thin and thick discs that are similar to the other methods, particularly the chronological method, but a larger fraction of thick disc stars in the plane and a higher density of halo stars than any other method.

All of the kinds of selection we have tested, with the exception of the abundance-based ones, would include an uncertainty zone if they were used only to measure the properties of the Galaxy. They would discard stars that fall close to the border of the selection of the components in order to reduce contamination. We do not do this because we want to compare the methods to each other, and our model works on component fractions, which

means the total number of stars in the analysis is important. If we were to exude stars that were difficult to categorise, our components would not be fractions of the total but fractions of the categorisable stars. Because of this, all our methods provide results with some amount of mixing.

From the work presented in this paper, we can draw the conclusion that the scale parameters of the Milky Way are not independent of the method of classification. Chemical abundances offer the most straightforward method for categorising stars, with age being a promising option as chronometric precision and coverage improve. Categorisations based on actions, while promising for their accessibility, suffer from blended populations that do not offer any clear limits for any component.

The lesson to learn from this is one that has already been voiced before by, e.g. Haywood et al. (2013), Hayden et al. (2017), and even Hunt & Vasiliev (2025), that clarity is required when talking about the components of the Milky Way disc. We would extend the advice of these authors even further, as we showed that it is not only the chemically and geometrically defined discs that are different, but that the discs are different regardless of which metric is used to define them. It is important to be aware of the potential effects a choice of definition can have on the components that are recovered.

4 Outlook

As the revolution in understanding of the dynamics of the Milky Way kicked off by *Gaia* continues and we gain more insight into the perturbed state the Galaxy is in, much work is needed both to understand the current state of the Milky Way, to map the features that exist, and to understand what caused them. By combining a precise observational inventory of the structures in the Milky Way with detailed simulations, we can hope to understand the present state of the Galaxy and the physical processes that have shaped it over time.

The Milky Way disc is in a dynamically active state and not very close to equilibrium. The global detection of the phase-space spiral, its measurable change in orientation with azimuth, its varying strength with angular momentum, and the presence of the two-armed version in a narrow range of angular momentum all show this. Independent investigations also show that the Milky Way disc hosts vertical corrugations, a warp, and numerous kinematic substructures. It seems likely that most, if not all, of these phenomena are related and share causes or driving mechanisms.

Looking ahead, there are clear reasons to be optimistic about progress in this field.

More data from ground-based surveys and future *Gaia* data releases. The observational landscape continues to improve at a remarkable pace. Future data releases from the *Gaia*

mission (DR4 and DR5, based on 5 and 10 years of data, respectively) will further improve our data on stellar positions, motions, and astrophysical parameters, delivering increased precision and expanding the time baseline for astrometric measurements. This will enable even more detailed studies of stellar kinematics and the dynamical substructure of the Milky Way. Complementing these improvements are ongoing and upcoming ground-based spectroscopic surveys, such as the 4MIDABLE-HR and LR surveys (Bensby et al. 2019; Chiappini et al. 2019), WEAVE (Jin et al. 2024), and others. They will provide radial velocities, chemical abundance, and astroseismology for millions of stars. Together, these data sets will fill gaps in our current knowledge by providing more data for all stellar populations. The combination of precise astrometry, radial velocities, chemical abundances, and other parameters promises to improve our understanding of Galactic components and uncover new structures that still await discovery.

Models and theory catching up to the data. The rapid progress in observations has created a situation where the fidelity and quantity of observations have outpaced the resolution of available models. Improvements in both the technical capabilities of models and the methodological construction of them can make models catch up to observations. The coming years are likely to see substantial progress in developing models that can better reproduce the fine-grained phase-space features observed by Gaia. Improved models will clarify how internal components and mechanisms, like the bar and its effects on the rest of the Galaxy, and external perturbations, such as the Sagittarius dwarf galaxy, influence the Galaxy and how they relate to and affect each other. We can already see the beginning of this with works like Tepper-García et al. (2025), who uses high-resolution, N-body and hydrodynamical simulations with a realistic ISM that interacts with a massive external perturber to investigate the formation and survival of phase spirals. As models improve, they will allow us to test hypotheses about the origin of the thin and thick discs, the formation of the bar and spiral arms, and the broader history of interactions that shaped the Milky Way. A closer alignment between theory and observation will not only explain the structures we see today but also provide greater predictive power for future discoveries.

The promise of GaiaNIR. The planned GaiaNIR mission bears the promise to revolutionise Galactic studies in a way comparable to, or even greater than, the original Gaia mission. By observing in the near-infrared, GaiaNIR will be able to probe regions of the Galaxy that are heavily obscured by dust in optical wavelengths. This includes large areas of the Galactic plane, the inner bulge, and the far side of the disc, regions that are crucial for a complete understanding of Galactic structure and dynamics but which are obscured in current surveys. The vertical line at Z=0 in Fig. 3.8 is an example of data that is affected by the presence of dust in the plane of the Galaxy. Access to these regions will allow for an unprecedented census of stars across the Milky Way, potentially providing the missing pieces required to build a more complete global dynamical model of the Galaxy. The very long baseline available by combining GaiaNIR with Gaia and other surveys will also give

the highest precision astrometric data ever, further enabling studies that have not previously been possible. Just as *Gaia* transformed our understanding of the Milky Way, *GaiaNIR* is likely to open up new directions in Galactic archaeology, enabling us to address long-standing questions about the distribution of dark matter, the formation of the bar and spiral arms, and the assembly history of the Galactic disc. (Hobbs & Høg 2018; Hobbs et al. 2021).

References

Abdurro'uf, Accetta, K., Aerts, C., et al. 2022, ApJS, 259, 35

Alinder, S., McMillan, P. J., & Bensby, T. 2023, A&A, 678, A46

Alinder, S., McMillan, P. J., & Bensby, T. 2024, A&A, 690, A15

Antoja, T., Helmi, A., Romero-Gómez, M., et al. 2018, Nature, 561, 360

Antoja, T., Ramos, P., García-Conde, B., et al. 2023, A&A, 673, A115

Athanassoula, E. 2005, MNRAS, 358, 1477

Bailer-Jones, C. A. L., Rybizki, J., Fouesneau, M., Demleitner, M., & Andrae, R. 2021, AJ, 161, 147

Belokurov, V., Erkal, D., Evans, N. W., Koposov, S. E., & Deason, A. J. 2018, MNRAS, 478, 611

Belokurov, V., Zucker, D. B., Evans, N. W., et al. 2006, ApJL, 642, L137

Bennett, M., Bovy, J., & Hunt, J. A. S. 2022, ApJ, 927, 131

Bensby, T., Alves-Brito, A., Oey, M. S., Yong, D., & Meléndez, J. 2011, ApJL, 735, L46

Bensby, T., Bergemann, M., Rybizki, J., et al. 2019, The Messenger, 175, 35

Bensby, T., Feltzing, S., & Lundström, I. 2003, A&A, 410, 527

Bensby, T., Feltzing, S., Lundström, I., & Ilyin, I. 2005, A&A, 433, 185

Bensby, T., Feltzing, S., & Oey, M. S. 2014, A&A, 562, A71

Bergbusch, P. A. & VandenBerg, D. A. 2001, ApJ, 556, 322

Bergemann, M., Sesar, B., Cohen, J. G., et al. 2018, Nature, 555, 334

Bessel, F. W. 1838, MNRAS, 4, 152

Binney, J. 2012, MNRAS, 426, 1324

Binney, J. & Merrifield, M. 1998, Galactic Astronomy (Princeton University Press)

Binney, J. & Sanders, J. L. 2016, Astronomische Nachrichten, 337, 939

Binney, J. & Schönrich, R. 2018, MNRAS, 481, 1501

Binney, J. & Tremaine, S. 2008, Galactic Dynamics: Second Edition (Princeton University Press)

Bland-Hawthorn, J., Sharma, S., Tepper-Garcia, T., et al. 2019, MNRAS, 486, 1167

Bland-Hawthorn, J. & Tepper-García, T. 2021, MNRAS, 504, 3168

Bonaca, A. & Price-Whelan, A. M. 2025, NewAR, 100, 101713

Bosma, A. 1978, PhD thesis, University of Groningen, Netherlands

Bournaud, F., Elmegreen, B. G., & Martig, M. 2009, ApJL, 707, L1

Bovy, J., Rix, H.-W., Liu, C., et al. 2012, ApJ, 753, 148

Bovy, J., Rix, H.-W., Schlafly, E. F., et al. 2016, ApJ, 823, 30

Burke, B. F. 1957, AJ, 62, 90

Casetti-Dinescu, D. I., Girard, T. M., Korchagin, V. I., & van Altena, W. F. 2011, ApJ, 728, 7

Cerqui, V., Haywood, M., Di Matteo, P., Katz, D., & Royer, F. 2023, A&A, 676, A108

Cheng, J. Y., Rockosi, C. M., Morrison, H. L., et al. 2012, ApJ, 752, 51

Cheng, X., Anguiano, B., Majewski, S. R., et al. 2020, ApJ, 905, 49

Chiappini, C., Minchey, I., Starkenburg, E., et al. 2019, The Messenger, 175, 30

Chung, C., Lee, Y.-W., & Pasquato, M. 2016, MNRAS, 456, L1

Cunha, M. S., Aerts, C., Christensen-Dalsgaard, J., et al. 2007, A&A Rv, 14, 217

Darragh-Ford, E., Hunt, J. A. S., Price-Whelan, A. M., & Johnston, K. V. 2023, ApJ, 955, 74

Das, P., Hawkins, K., & Jofré, P. 2020, MNRAS, 493, 5195

Dehnen, W. 1999, in Astronomical Society of the Pacific Conference Series, Vol. 182, Galaxy Dynamics - A Rutgers Symposium, ed. D. R. Merritt, M. Valluri, & J. A. Sell-wood, 297

Dwek, E., Arendt, R. G., Hauser, M. G., et al. 1995, ApJ, 445, 716

El-Badry, K., Rix, H.-W., Quataert, E., et al. 2023, MNRAS, 518, 1057

Foreman-Mackey, D., Hogg, D. W., Lang, D., & Goodman, J. 2013, PASP, 125, 306

Frankel, N., Bovy, J., Tremaine, S., & Hogg, D. W. 2023, MNRAS, 521, 5917

Fuhrmann, K. 1998, A&A, 338, 161

Gaia Collaboration, Antoja, T., McMillan, P. J., et al. 2021, A&A, 649, A8

Gaia Collaboration, Brown, A. G. A., Vallenari, A., et al. 2018, A&A, 616, A1

Gaia Collaboration, Brown, A. G. A., Vallenari, A., et al. 2016a, A&A, 595, A2

Gaia Collaboration, David, P., Mignard, F., et al. 2023a, A&A, 680, A37

Gaia Collaboration, Drimmel, R., Romero-Gómez, M., et al. 2023b, A&A, 674, A37

Gaia Collaboration, Krone-Martins, A., Ducourant, C., et al. 2024a, A&A, 685, A130

Gaia Collaboration, Panuzzo, P., Mazeh, T., et al. 2024b, A&A, 686, L2

Gaia Collaboration, Prusti, T., de Bruijne, J. H. J., et al. 2016b, A&A, 595, A1

Gaia Collaboration, Vallenari, A., Brown, A. G. A., et al. 2023c, A&A, 674, A1

Gilliland, R. L., Brown, T. M., Christensen-Dalsgaard, J., et al. 2010, PASP, 122, 131

Gilmore, G. & Reid, N. 1983, MNRAS, 202, 1025

Glazebrook, K., Nanayakkara, T., Schreiber, C., et al. 2024, Nature, 628, 277

Goodman, J. & Weare, J. 2010, Communications in Applied Mathematics and Computational Science, 5, 65

Grand, R. J. J., Kawata, D., Belokurov, V., et al. 2020, MNRAS, 497, 1603

Guo, R., Shen, J., Li, Z.-Y., Liu, C., & Mao, S. 2022, ApJ, 936, 103

Halley, E. 1717, Philosophical Transactions of the Royal Society of London Series I, 30, 736

Hawkins, K., Jofré, P., Masseron, T., & Gilmore, G. 2015, MNRAS, 453, 758

Hayden, M. R., Recio-Blanco, A., de Laverny, P., Mikolaitis, S., & Worley, C. C. 2017, A&A, 608, L1

Haywood, M., Di Matteo, P., Lehnert, M. D., Katz, D., & Gómez, A. 2013, A&A, 560, A109

Helmi, A. 2008, A&A Rv, 15, 145

Helmi, A., Babusiaux, C., Koppelman, H. H., et al. 2018, Nature, 563, 85

Henderson, T. 1839, MNRAS, 4, 168

Hobbs, D., Brown, A., Høg, E., et al. 2021, Experimental Astronomy, 51, 783

Hobbs, D. & Høg, E. 2018, in IAU Symposium, Vol. 330, Astrometry and Astrophysics in the Gaia Sky, ed. A. Recio-Blanco, P. de Laverny, A. G. A. Brown, & T. Prusti, 67–70

Høg, E., Fabricius, C., Makarov, V. V., et al. 2000, A&A, 355, L27

Huggins, W. 1868, Philosophical Transactions of the Royal Society of London Series I, 158, 529

Hunt, J. A. S., Price-Whelan, A. M., Johnston, K. V., & Darragh-Ford, E. 2022, MNRAS, 516, L7

Hunt, J. A. S. & Vasiliev, E. 2025, NewAR, 100, 101721

Ibata, R., Malhan, K., Martin, N., et al. 2021, ApJ, 914, 123

Ibata, R., Malhan, K., Tenachi, W., et al. 2024, ApJ, 967, 89

Ibata, R. A., Gilmore, G., & Irwin, M. J. 1994, Nature, 370, 194

Ibata, R. A., Gilmore, G., & Irwin, M. J. 1995, MNRAS, 277, 781

Ibata, R. A., Irwin, M. J., Lewis, G. F., Ferguson, A. M. N., & Tanvir, N. 2003, MNRAS, 340, L21

Immeli, A., Samland, M., Gerhard, O., & Westera, P. 2004, A&A, 413, 547

Jin, S., Trager, S. C., Dalton, G. B., et al. 2024, MNRAS, 530, 2688

Jónsson, V. H. & McMillan, P. J. 2024, A&A, 688, A38

Jørgensen, B. R. & Lindegren, L. 2005, A&A, 436, 127

Jurić, M., Ivezić, Ž., Brooks, A., et al. 2008, ApJ, 673, 864

Kapteyn, J. C. & Weersma, H. A. 1910, Publications of the Kapteyn Astronomical Laboratory Groningen, 24, 1

Katz, D., Gómez, A., Haywood, M., Snaith, O., & Di Matteo, P. 2021, A&A, 655, A111

Katz, D., Sartoretti, P., Guerrier, A., et al. 2023, A&A, 674, A5

Kerr, F. J., Hindman, J. V., & Carpenter, M. S. 1957, Nature, 180, 677

Khoperskov, S., Haywood, M., Snaith, O., et al. 2021, MNRAS, 501, 5176

Kormendy, J. & Kennicutt, Jr., R. C. 2004, ARA&A, 42, 603

Kruijssen, J. M. D., Pfeffer, J. L., Chevance, M., et al. 2020, MNRAS, 498, 2472

Kushniruk, I., Schirmer, T., & Bensby, T. 2017, A&A, 608, A73

Lambas, D. G., Alonso, S., Mesa, V., & O'Mill, A. L. 2012, A&A, 539, A45

Laporte, C. F. P., Belokurov, V., Koposov, S. E., Smith, M. C., & Hill, V. 2020a, MNRAS, 492, L61

Laporte, C. F. P., Famaey, B., Monari, G., et al. 2020b, A&A, 643, L3

Laporte, C. F. P., Gómez, F. A., Besla, G., Johnston, K. V., & Garavito-Camargo, N. 2018, MNRAS, 473, 1218

Laporte, C. F. P., Johnston, K. V., & Tzanidakis, A. 2019a, MNRAS, 483, 1427

Laporte, C. F. P., Koposov, S. E., & Belokurov, V. 2022, MNRAS, 510, L13

Laporte, C. F. P., Minchey, I., Johnston, K. V., & Gómez, F. A. 2019b, MNRAS, 485, 3134

Leung, H. W. & Bovy, J. 2019, MNRAS, 483, 3255

Li, C., Siebert, A., Monari, G., Famaey, B., & Rozier, S. 2023, MNRAS, 524, 6331

Lin, J., Li, Z.-Y., Guo, R., et al. 2025, ApJ, 988, 254

López-Corredoira, M., Allende Prieto, C., Garzón, F., et al. 2018, A&A, 612, L8

Lundmark, K. 1930, Meddelanden fran Lunds Astronomiska Observatorium Serie I, 125, 1

Lynden-Bell, D. & Lynden-Bell, R. M. 1995, MNRAS, 275, 429

Mackereth, J. T., Bovy, J., Leung, H. W., et al. 2019, MNRAS, 489, 176

Mackereth, J. T., Bovy, J., Schiavon, R. P., et al. 2017, MNRAS, 471, 3057

Majewski, S. R., Schiavon, R. P., Frinchaboy, P. M., et al. 2017, AJ, 154, 94

Martig, M., Minchev, I., Ness, M., Fouesneau, M., & Rix, H.-W. 2016, ApJ, 831, 139

Martínez-Delgado, D., Gabany, R. J., Crawford, K., et al. 2010, AJ, 140, 962

Massari, D., Breddels, M. A., Helmi, A., et al. 2018, Nature Astronomy, 2, 156

Massari, D., Koppelman, H. H., & Helmi, A. 2019, A&A, 630, L4

Matteucci, F. & Greggio, L. 1986, A&A, 154, 279

McMillan, P. J. 2017, MNRAS, 465, 76

Minchey, I., Martig, M., Streich, D., et al. 2015, ApJL, 804, L9

Mori, M. & Umemura, M. 2006, Nature, 440, 644

Nepal, S., Chiappini, C., Pérez-Villegas, A., et al. 2025, arXiv e-prints, arXiv:2507.06863

Ness, M. & Lang, D. 2016, AJ, 152, 14

Newberg, H. J., Yanny, B., Rockosi, C., et al. 2002, ApJ, 569, 245

Nordlander, T. & Lind, K. 2017, A&A, 607, A75

Orkney, M. D. A., Laporte, C. F. P., Grand, R. J. J., et al. 2022, MNRAS, 517, L138

Perryman, M. 2009, Astronomical Applications of Astrometry: Ten Years of Exploitation of the Hipparcos Satellite Data (Cambridge University Press)

Perryman, M. A. C., Hassan, H., Batut, T., et al., eds. 1989, The Hipparcos mission. Prelaunch status. Volume I: The Hipparcos satellite., Vol. 1

Perryman, M. A. C., Lindegren, L., Kovalevsky, J., et al. 1997, A&A, 323, L49

Pinsonneault, M. H., Elsworth, Y., Epstein, C., et al. 2014, ApJS, 215, 19

Planelles, S., Schleicher, D. R. G., & Bykov, A. M. 2015, SSRv, 188, 93

Poggio, E., Khanna, S., Drimmel, R., et al. 2025, A&A, 699, A199

Recio-Blanco, A., de Laverny, P., Palicio, P. A., et al. 2023, A&A, 674, A29

Reddy, B. E., Tomkin, J., Lambert, D. L., & Allende Prieto, C. 2003, MNRAS, 340, 304

Rix, H.-W. & Bovy, J. 2013, A&A Rv, 21, 61

Rocha-Pinto, H. J., Majewski, S. R., Skrutskie, M. F., Crane, J. D., & Patterson, R. J. 2004, ApJ, 615, 732

Rubin, V. C. & Ford, Jr., W. K. 1970, ApJ, 159, 379

Salaris, M., Pietrinferni, A., Piersimoni, A. M., & Cassisi, S. 2015, A&A, 583, A87

Schönrich, R. & Binney, J. 2009, MNRAS, 399, 1145

Sellwood, J. A. & Binney, J. J. 2002, MNRAS, 336, 785

Sheffield, A. A., Price-Whelan, A. M., Tzanidakis, A., et al. 2018, ApJ, 854, 47

Slater, C. T., Bell, E. F., Schlafly, E. F., et al. 2014, ApJ, 791, 9

Soderblom, D. R. 2010, ARA&A, 48, 581

Tanikawa, A., Hattori, K., Kawanaka, N., et al. 2023, ApJ, 946, 79

Tepper-García, T., Bland-Hawthorn, J., Bedding, T. R., Federrath, C., & Agertz, O. 2025, MNRAS, 542, 1987

Tremaine, S., Frankel, N., & Bovy, J. 2023, MNRAS, 521, 114

Vasiliev, E. 2019, MNRAS, 482, 1525

Wang, C., Huang, Y., Yuan, H. B., et al. 2019, ApJL, 877, L7

Wang, W., Cantalupo, S., Pensabene, A., et al. 2025, Nature Astronomy, 9, 710

Westerhout, G. 1957, BAN, 13, 201

Widmark, A., Laporte, C., & de Salas, P. F. 2021a, A&A, 650, A124

Widmark, A., Laporte, C. F. P., de Salas, P. F., & Monari, G. 2021b, A&A, 653, A86

Widmark, A., Laporte, C. F. P., & Monari, G. 2022, A&A, 663, A15

Widrow, L. M. 2023, MNRAS, 522, 477

Widrow, L. M., Barber, J., Chequers, M. H., & Cheng, E. 2014, MNRAS, 440, 1971

Wolf, M. 1919, Veroeffentlichungen der Badischen Sternwarte zu Heidelberg, 10, 195

Wynn-Williams, C. G. 2016, Surveying the Skies: How Astronomers Map the Universe, Astronomers' Universe Ser (Cham: Springer International Publishing AG)

Xiang, M. & Rix, H.-W. 2022, Nature, 603, 599

Xu, Y., Newberg, H. J., Carlin, J. L., et al. 2015, ApJ, 801, 105

Yoshii, Y. 2013, in Planets, Stars and Stellar Systems. Volume 5: Galactic Structure and Stellar Populations, ed. T. D. Oswalt & G. Gilmore, Vol. 5 (Springer Science+Business Media), 393

Scientific publications

Author contributions

Paper I

Investigating the amplitude and rotation of the phase spiral in the Milky Way outer disc S. Alinder, P. J. McMillan, T. Bensby

Astronomy & Astrophysics, Volume 678, id.A46, 17 pp. (2023)

I led the analysis of the data and development of the model used to quantify the phase spiral. Paul McMillan contributed the probability function used to fit the spiral. I led the writing of the paper with comments from Thomas Bensby and Paul McMillan.

Paper II

Limitations and rotation of the two-armed phase spiral in the Milky Way stellar disc S. Alinder, P. J. McMillan, T. Bensby Astronomy & Astrophysics, Volume 690, id.A15, 11 pp. (2024)

I led the further development of the model originally developed for Paper I for expanded use and led the analysis of the data. I led the writing of the paper with comments from Thomas Bensby and Paul McMillan.

Paper III

Vertical scale heights of the Milky Way thick and thin discs using different selection methods

S. Alinder, T. Bensby, P. J. McMillan Astronomy & Astrophysics, to be submitted

The original idea for this project came from Thomas Bensby. I developed the categorisation methods and led the analysis of the data. Paul McMillan made the probability function used to fit the disc model. I then led the writing of the paper with comments from Thomas Bensby and Paul McMillan.